

Taking Into Account Of The Non-Linearities Of The Magnetic Material For The Characterization In Steady State Under Presumed Sinusoidal Voltage Of The Behavior Of A Single-Phase Magnetic Circuit

J.F. BRUDNY, C. DEMIAN

Univ. Artois, UR 4025, Laboratoire Systèmes Electrotechniques et Environnement (LSEE),
Béthune, F-62400, France

ABSTRACT

The developments presented consider, via μ_r , the non-linearities of the magnetic material to determine, based on the conventional equivalent scheme, the equations which characterize the operation in steady state of a single-phase Magnetic Circuit (MC) supplied with a presumed sinusoidal voltage. If some results have already been the subject of a scientific publication, this new article is characterized by the numerous experimental exploitations. These validate all the specific equations applicable whether or not the MC is affected by saturation. On the other hand, the exploitation of these equations makes it possible to access practical information concerning this MC which is difficult to obtain by other methods. The original aspects resulting from this analysis are at several levels.

- Establishment, on the basis of a semi-analytical method of investigation already exposed, of the complete system of equations governing the behavior of the MC.
- Presentation of a simple and fast procedure for the characterization of the impedance of the grid which supplies this MC.
- Identification of the iron loss analytical model and quantification of the associated variable resistive elements.
- Extension to the determinations of the experimental anhysteretic and $\mu_r(b)$ characteristics of the magnetic material.
- Analysis of the impacts of these specific formulations on the fundamental iron losses determined using dedicated devices such as Epstein frame.

Keywords: Magnetic circuit; Saturation; Permeability; Iron losses; Magnetizing inductance active behavior.

Date of Submission: 03-07-2023

Date of acceptance: 14-07-2023

I. INTRODUCTION

Generally, a transformer is sized for a peak flux density (\hat{b}) level which does not subject the magnetic material to excessively high saturations. These are around 1,2T for NO and 1,5T for GO. Under these conditions, the harmonic distortion on the no-load current is relatively controlled, allowing the notion of Equivalent Sinusoidal Current (ESC) to be exploited. On the other hand, in many cases, this transformer is supplied with an imposed rms sinusoidal voltage leading to consider that the relative permeability μ_r is identified with a constant. This approach turns out to be very practical for characterizing load operations on linear or non-linear receivers. The main handicap of this way of proceeding is linked to the nature of μ_r which is a quantity that can present, on the scale of a period,

significant variations. These latter are sometimes vaguely mentioned to simply justify, with the help of a graphic plot, certain physical phenomena linked to saturation, such as the peak which affects the current absorbed in no-load condition [1]. Regarding saturation, the scientific literature reveals many articles. There are those which deal with theoretical aspects [2-5], others which take it into account to justify certain behaviors [6-8] and those that consider this phenomenon from a metrological point of view [9-11]. However, few analyzes [12] deal with the subject of saturation from the angle of the practical characterization of the MC operating. This paper proposes to fill this gap by presenting, on the basis of the conventional equivalent scheme [13], the system of equations which governs, in steady state under presumed sinusoidal voltage, the behavior of such a MC. The validation of this theory

will simply be based on the experimental results obtained in the context of classical tests, at the level of which certain anomalies, which everyone can see, are, with the ESC notion, quite simply ignored.

From a pragmatic point of view, this analysis results from eco-design considerations for the sizing of such a MC in the context of specific applications. The objective is, at the desired power and given sheet quality, to increase the \hat{b} values in order to reduce the volumes of iron and copper by limiting the excessive degradation of the energy performance of these devices. Implicitly, this supposes a better control of the behaviors related to the saturation as evoked in [11]. A second aspect, not negligible, concerns the definition of specific functions whose very principle is based on saturation [14-18].

The analysis already presented on the subject [13] shows that this MC, supplied with a perfectly sinusoidal voltage, is characterized, for \hat{b} values greater than 0,8T, by negative active and reactive power harmonic components. The justification of their existence was mainly based on the analysis of the results obtained using a Semi-Analytical Method that we developed and designated by the acronym SAM. These powers are essentially dependent on the distortions induced by the natural current harmonics which, through the voltage drops they cause, affect the behavior of the MC. As a result, what can be qualified at this stage as anomalies affects this MC whatever the value of \hat{b} . This paper differs from [13] by the consequent experimental investigations which have been carried out for different values of \hat{b} . The latter, associated with the specific relations which characterize the MC operating, make it possible to predetermine all the parameters which characterize the elements of its equivalent scheme associated with a modeling of its supply grid. The question may arise of the interest of carrying out a characterization of the fundamental iron losses or of $\mu_r(b)$ because this information can be extracted from the data that the metallurgists, producers of magnetic steels, make available on their site. In fact, the analysis carried out shows that the information obtained differs significantly from what can be deduced from the manufacturer's data. This can, in part, be justified by the experimental conditions, but also by the fact of exploiting relations that are not quite adapted and which come under the ESC notion.

This paper first summarizes the general elements necessary for the developments that will be exposed. The following paragraph, on the basis of SAM presented in the appendix, exposes the rather particular relations which govern the behavior of an MC. Paragraph IV concerns the experimental data as well as the protocol implemented to exploit them. Paragraph V, on the basis of these data, characterizes the components of the equivalent scheme of this MC associated with its supply grid. The comparison of the experimental results with those deduced from SAM applied to a given experimental case, will be the subject of paragraph VI. These developments will also make it possible to raise a problem which probably affects the information obtained using dedicated devices to evaluate, in particular, the fundamental iron losses [19-22].

This paper is based on a relatively large number of numerical data resulting from both experiments and developed procedures. These have been grouped together in a Digital File (DF). Only certain results of DF appear in this paper.

II. GENERAL CONSIDERATIONS.

II.1) Presentation of the MC.

II.1.1) Technical description of the MC.

This MC, shown in Fig. 1, has a toroidal magnetic core produced by an assembly of sheets cut according to crowns in a magnetic material considered as quasi isotropic: the NO Power Core M400-50A. This core carries 3 windings: a primary, a secondary and a measurement winding. Each winding has $n=100$ turns so that the transformation ratios between these windings are identified as 1. Primary and secondary windings are made with a $2,5\text{mm}^2$ copper wire. The measurement winding, made with wire of very small section, makes it possible, by integration of the emf "e" which appears at its terminals, to determine "b". The primary winding is supplied by a voltage "v" whose fundamental evolves at a constant frequency $f=50\text{Hz}$ (period T, pulsation ω).

The MC schematic representation, given in Fig. 2, specifies the geometric variables which characterize it: $R_{\text{ext}}=0,1\text{m}$, $R_{\text{int}}=0,0815\text{m}$. This defines: $W=0,0185\text{m}$, $R_{\text{mean}}=0,09075\text{m}$ leading to an average length of the field lines $L_{\text{MC}}=0,57\text{m}$. The MC is made up of a stack of 54 sheets 0,5mm thick defining: $E_{\text{MC}}=0,027\text{m}$ and the MC section: $S_{\text{MC}}=4,995*10^{-4}\text{m}^2$.

II.1.2) Equivalent Scheme. This paper is only concerned with the no-load operation of this MC which is shown in Fig. 3 through its conventional equivalent scheme connected to an imperfect supply. Fig. 3 also shows the notations used. r_p and l_p respectively define the resistance and the leakage inductance of the primary winding, the entity R_{il} , of resistive nature, characterizes the iron losses and L_μ corresponds to the magnetizing inductance dependent on operating conditions. The

whose location is not known, which delivers a sinusoidal voltage v_G transmitted to the MC by a line whose impedance consists of the series association of r_G and l_G . r_p , l_p , r_G and l_G are assumed to identify with constants defining $r = r_G + r_p$, $l = l_G + l_p$ and the réactances $x_p = l_p \omega$, $x_G = l_G \omega$, $x = x_G + x_p = l \omega$. These quantities constitute the line components. R_{il} and L_μ are the magnetic block components.



Fig.1: Toroidal MC

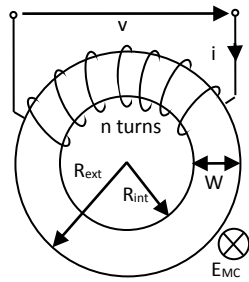


Fig.2: MC schematic representation

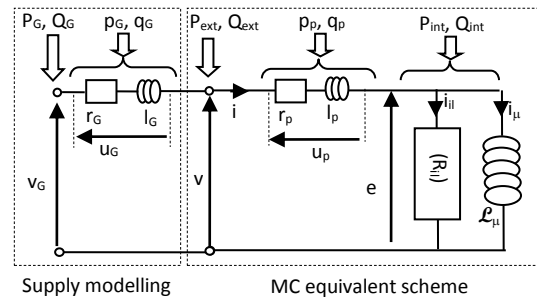


Fig. 3: MC and its supply

MC is supplied by an infinite power generator,

II.1.3) MC elementary characterization. Classical investigations, using ESC notion, make it possible to characterize certain elements. The no-load test for $V=10,28V$ ($\hat{b} \approx 1T$) leads to an rms current of 0,67A and iron losses of 3,32W (value close to that determined from the manufacturer data). It can be deduced that the R_{il} which symbolizes the fundamental iron losses is of the order of $31,8\Omega$ and that the reactance $X_\mu=L_\mu\omega$ is close to $17,5\Omega$. The short-circuit test defines $r_p=0,31\Omega$ and x_p very low compared to r_p without being able to make a numerical estimate other than: $x_p=0$.

II.2) Notations used. Relationships exploited. Conventions.

II.2.1) Notations used. An electric or magnetic "y" variable at a point in the scheme of Fig. 3, is characterized by its temporal expression $y(t)$ on "T" defined by a sequence of points regularly spaced by Δt . A Fourier Series FS(y) defined by :

$$FS(y) = \sum_k \hat{y}_k \cos(k\omega t - /y_k /)$$

(1)

is associated with $y(t)$ where, unless otherwise specified, k takes all odd values (1, 3, 5, ...). $\hat{y}_k = Y_k \sqrt{2}$ represents the peak value of this sinusoidal component of Y_k rms value which presents, with respect to the chosen time reference, a phase $/y_k /$ at time $t=0$. As the counterclockwise direction is retained to positively count the phases, the phase shift of y'_k with respect to y_k , denoted $/y'_k / y_k /$, is expressed by:

$$/y'_k / y_k / = /y'_k / - /y_k /$$

(2)

The transition from one formulation to another does not pose any particular difficulty.

II.2.2) Relationships used. These relations are derived from the basic theory of electromagnetism which considers that the flux generated by the primary winding comprises two components:

- the main component ϕ which circulates only in the magnetic core,
- the leakage flux, which largely closes in the air, taken into account with l_p at the level of Fig. 3, whose contribution to the definition of ϕ is neglected.

Assuming "b" uniform distribution on S_{MC} , "b" and "e" are linked by: $e = nS_{MC} \frac{db}{dt}$, defining $\hat{b}_k = \hat{e}_k / (k\omega nS_{MC})$ and therefore $\hat{\phi}_k = \hat{b}_k S_{MC}$. The $\mu_r(b)$ characteristic defines μ_r which leads to the magnetic

core reluctance \mathfrak{R} : $\mathfrak{R} = L_{MC} / \mu_0 \mu_r S_{MC}$. The relationship $b = \mu_r \mu_0 H$ with $\mu_0 = 4\pi 10^{-7} \text{H/m}$, by introducing the constant K : $K = L_{MC} / \eta \mu_0$, leads to :

$$\mu_r = Kb / i_\mu$$

(3)

Ampère theorem: $n i_\mu = \mathfrak{R} \phi$ define i_μ . ϕ leads to the main flux ψ linked by the primary winding: $\psi = n \phi$ defining the L_μ magnetizing inductance: $\mathcal{L}_\mu = \psi / i_\mu$. The i_μ expression leads to: $\mathcal{L}_\mu = n^2 / \mathfrak{R}$.

The i_{il} determination requires considering a model to characterize the iron losses which will be assumed to be dependent only on "b". For that, a set of R_{ilk} resistors will be associated with the R_{il} block in Fig. 3 defining i_{il} by:

$$i_{il} = \sum_k e_k / R_{ilk}$$

(4)

As: $i = i_{il} + i_\mu$, it comes $u_p = r_p i + l_p \frac{di}{dt}$, $u_G = r_G i + l_G \frac{di}{dt}$ and: $v_G = e + u_p + u_G$.

Note: Some justifications will require a minimum of mathematical developments that will use FSs. For example, if L_μ is proportional to μ_r , i_μ involves the μ_r inverse. Expressing i_μ with the inverse of $FS(\mu_r)$ is not without problems to establish certain properties. It follows that when determining μ_r from "b", it will also proceed to the determination of its inverse $\eta_r = 1/\mu_r$ so that $FS(1/\mu_r)$ will be identified with $FS(\eta_r)$. $FS(\mu_r)$ and $FS(\eta_r)$, will include an average value and harmonics of even ranks $2h$, h taking all integer values ($h=1, 2, 3, \dots$). It results μ_r and η_r are given by the formulations:

$$\left. \begin{aligned} \mu_r &= \langle \mu_r \rangle + \sum_h \hat{\mu}_{r2h} \cos(2h\omega t - / \mu_{r2h} /) \\ \eta_r &= \langle \eta_r \rangle + \sum_h \hat{\eta}_{r2h} \cos(2h\omega t - / \mu_{r2h} /) \end{aligned} \right\}$$

(5)

Regarding the variables that appear in Fig. 3, the following terminology will be used:

- external variables: variables directly or indirectly accessible to the measurements, these are v , i , e and b ,
- internal variables: variables not accessible to measurements such as i_{il} , i_μ but also u_p , u_G and v_G .

The active P and reactive Q powers which appear at a given point in this scheme satisfy the equalities:

$$\left. \begin{aligned} P &= \sum_k P_k \\ Q &= \sum_k Q_k \end{aligned} \right\}$$

(6)

P and Q represent the global powers defined, relative to P , of the integration of the instantaneous power given by the product of a voltage and a current. P_k and Q_k are the powers carried by the harmonics resulting from the classic sinusoidal relationships. These powers will be counted positively when they are conveyed from the supply to the MC and negatively when the transit takes place in the opposite direction.

III. MAIN RELATIONSHIPS CHARACTERIZING THE MC OPERATING.

These equations take into account the non-linearities of the magnetic material so that they are valid $\forall \hat{b}_1$. The problem comes from the fact that certain behaviors, in particular that of L_μ , are

difficult to predict making impossible to formulate easily, without prior hypothesis, these equations (hence the ESC notion). It was only after having developed and exploited a Semi Analytical Method (SAM) of analysis, that it was possible to establish this particular system of equations. SAM numerically exploits, using Excel, the previous relationships. As SAM's presentation has already been the subject of a scientific publication [13], its presentation has been transferred to appendix A. Two particularities deserve to be mentioned.

- This system of equations is based on the conventional structure of the equivalent scheme of this MC (see Fig. 3) whereas in [23], the authors adapt the structure of this scheme so as to be able to apprehend, according to them, in a more reliable way the aspects related to saturation.

- The principle implemented at SAM level requires imposing the input variable, in this case the supply voltage. Our analyzes at this stage consider that it is sinusoidal. Under these conditions, it is perfectly possible to impose sinusoidal "v". In this article, as the objective is to compare the experimental results with those deduced from SAM, it becomes much more difficult in practice to satisfy this condition imposed on "v". Indeed, despite the precautions taken at the level of the power supply device (signal generator associated with an a power amplifier), harmonics, even if they are low amplitudes, will always disturb "v" with regard to

the internal impedance, also weak as it is, that this device presents but also the impedance of the upstream grid. This is the reason why the implementation of SAM will be carried out by considering the imperfections of the power supply in accordance with the representation of Fig. 3 and the remarks made in II.1.2.

This appendix A also presents, by considering a theoretical case, the numerical results obtained with SAM, referenced SAM_{Th}, grouped in TA2. These could be considered as elements of validation and, if necessary, of justification during the presentation of some of the equations.

III.1) Theoretical expressions of i_{μ} and its components.

Ampère's theorem, noting: $K_{MC} = \mu_0 S_{MC} (n)^2 / L_{MC}$ and taking into account FS(η_r), leads to:

$$i_{\mu} = \left[\langle \eta_r \rangle + \sum_h \hat{\eta}_{r2h} \cos(2h\omega t - / \eta_{r2h} /) \right] \left[\sum_k \frac{\hat{e}_k}{k} \cos(k\omega t - / e_k / - \frac{\pi}{2}) \right] / K_{MC} \omega \quad (7)$$

(7) shows that i_{μ} is composed of two sets of terms. The first, defining i'_{μ} , is a function of $\langle \eta_r \rangle$, the second, i''_{μ} , is dependent on the 2h order harmonics of η_r . Hence, $\forall k$, the equality:

$$i_{\mu k} = i'_{\mu k} + i''_{\mu k} \quad (8)$$

Therefore, $\forall k$, $P_{\mu k}$ and $Q_{\mu k}$ can expressed as:

$$\left. \begin{aligned} P_{\mu k} &= P'_{\mu k} + P''_{\mu k} \\ Q_{\mu k} &= Q'_{\mu k} + Q''_{\mu k} \end{aligned} \right\} \quad (9)$$

$P'_{\mu k}$ and $Q'_{\mu k}$ are associated to $i'_{\mu k}$, $P''_{\mu k}$ and $Q''_{\mu k}$ to $i''_{\mu k}$.

• Concerning $i'_{\mu k}$ il comes:

$$i'_{\mu k} = \frac{\langle \eta_r \rangle}{K_{MC} \omega} \frac{\hat{e}_k}{k} \cos(k\omega t - / e_k / - \frac{\pi}{2}) \quad (10)$$

As $/i'_{\mu k}/e_k/ = \pi/2$, it results that $i'_{\mu k}$ it is at the origin only of $Q'_{\mu k}$ since:

$$P'_{\mu k} = 0 \quad \forall k \quad (11)$$

Like $P_{\mu k} = P''_{\mu k} \quad \forall k$, only $P_{\mu k}$ will be used hereafter from a terminological point of view.

• i''_{μ} results from a composition of terms with ranks 2h of η_r and ranks "k" of "e". For a matter of homogeneity, in order to characterize $i''_{\mu k}$ always using the rank "k", the rank k' will be introduced to define "e" knowing that k' plays the same role as "k". Under these conditions i''_{μ} results from the expression:

$$i''_{\mu} = \left[\sum_h \hat{\eta}_{r2h} \cos(2h\omega t - / \eta_{r2h} /) \right] \left[\sum_k \frac{\hat{e}_{k'}}{k'} \cos(k'\omega t - / e_{k'} / - \frac{\pi}{2}) \right] / K_{MC} \omega \quad (12)$$

which can also be written as:

$$i''_{\mu} = \frac{1}{2K_{CM} \omega} \sum_h \sum_{k'} \hat{\eta}_{r2h} \frac{\hat{e}_{k'}}{k'} \left\{ \cos[(2h+k')\omega t - / \eta_{r2h} / - / e_{k'} / - \frac{\pi}{2}] + \cos[(2h-k')\omega t - / \eta_{r2h} / + / e_{k'} / + \frac{\pi}{2}] \right\} \quad (13)$$

(k-2h) can, depending on the values of k and h, be positive or negative. To remove any ambiguity when this quantity occurs at the levels of \hat{e}_k or $/e_k/$, the absolute value $|k-2h|$ is introduced as well as the function "sgn" defined by:

$$\left. \begin{aligned} \operatorname{sgn}(k-2h) &= 1 \quad \text{if } (k-2h) > 0 \\ \operatorname{sgn}(k-2h) &= -1 \quad \text{if } (k-2h) < 0 \end{aligned} \right\}$$

(14)

Under these conditions, $i''_{\mu k}$ is expressed by:

$$i''_{\mu k} = \frac{1}{2K_{MC}\omega} \sum_h \hat{\eta}_{2h} \left\{ \frac{\hat{e}_{|k-2h|}}{(k-2h)} \sin\left[k\omega t - / \eta_{r2h} / - \operatorname{sgn}(k-2h) / e_{|k-2h|} / \right] + \frac{\hat{e}_{(k+2h)}}{(k+2h)} \sin\left[k\omega t + / \eta_{2h} / - / e_{(k+2h)} / \right] \right\}$$

(15)

For given "k", for values of "h" such that $(k+2h) > 21$, considering the limits imposed on "k" and "h", the second term of (15) may not exist. This may be source of errors if $i''_{\mu k}$ is defined with low maximum values of "k" and "h" [13].

III.2) Balance of powers at the level of external variables

In order to define the rules which govern the MC operating, the simplest thing is to carry out a balance sheet of the powers which appear at the various points of Fig. 3 knowing that:

- the principle of conservation of active and reactive powers (Boucherot's theorem) is satisfied [13],
- the losses $p_{Gk} = r_G I_k^2$, $p_{pk} = r_p I_k^2$, $p_k = r I_k^2$ and P_{ilk} as well as $q_{Gk} = kx_G I_k^2$, $q_{pk} = kx_p I_k^2$ et $q_k = kx I_k^2$ are positive quantities (see Part 3 of TA2).

By considering this MC at the level of v_G , it comes:

$$\left. \begin{aligned} P_{Gk} &= P_{extk} + p_{Gk} \\ Q_{Gk} &= Q_{extk} + q_{Gk} \end{aligned} \right\} \quad \forall k$$

(16)

As P_{Gk} and Q_{Gk} for $k > 1$ are zero, it can be deduced that :

$$\left. \begin{aligned} P_{extk} &= -p_{Gk} \\ Q_{extk} &= -q_{Gk} \end{aligned} \right\} \quad \text{for } k > 1$$

(17)

P_{extk} and Q_{extk} are, for $k > 1$, negative or zero (lines 31 and 32 of TA2). By developing P_{extk} and Q_{extk} , (16) is written:

$$\left. \begin{aligned} P_{Gk} &= P_{intk} + p_{pk} + p_{Gk} \\ Q_{Gk} &= Q_{intk} + q_{pk} + q_{Gk} \end{aligned} \right\} \quad \forall k$$

(18)

equalities which show, for $k > 1$, that P_{intk} and Q_{intk} are negative or zero (lines 36 and 37 of TA2) with:

$$\left. \begin{aligned} P_{intk} &= -(p_{pk} + p_{Gk}) = -p_k \\ Q_{intk} &= -(q_{pk} + q_{Gk}) = -q_k \end{aligned} \right\} \quad \text{pour } k > 1$$

(19)

The validity of the first relation of (19) is verified by considering lines 36 and 33 of TA2. Concerning the second relation of (19), it suffices to refer to lines 37 and 34. These equalities show that the harmonic powers at the level of the external variables ($k > 1$) allow, by considering FS(i), to quantify the line components numerically.

III.3) Balance of the powers on the level of the internal variables.

At the internal level, must be satisfied the equalities:

$$\left. \begin{aligned} P_{int\ k} &= P_{ilk} + P_{\mu k} \\ Q_{int\ k} &= Q_{\mu k} \end{aligned} \right\} \forall k$$

(20)

Given (19), it can be deduced that:

$$\left. \begin{aligned} P_{\mu k} &= -(p_k + P_{ilk}) \\ Q_{\mu k} &= -q_k \end{aligned} \right\} \text{ pour } k > 1$$

(21)

$P_{\mu k}$ and $Q_{\mu k}$ are therefore, for $k > 1$, negative or zero as appears in lines 40 and 41 of TA2.

III.3.1) Active powers. As for any pure inductance, the active power P_{μ} characterizing L_{μ} must theoretically be zero leading therefore to satisfy the equality: $P_{\mu} = \sum_k P_{\mu k} = 0$, that to say:

$$P_{\mu 1} = - \sum_{k(k>1)} P_{\mu k}$$

(22)

Line 40 of TA2 shows that (22) is satisfied. If the $P_{\mu k}$ are defined with more decimals, it appears that P_{μ} amounts to less than 0,01% of $P_{\mu 1}$, a percentage which results from numerical inaccuracies.

(22) and the first equality of (21) specify that $P_{\mu 1} = \sum_{k(k>1)} (p_k + P_{ilk})$ is a positive quantity. It follows that for $k > 1$,

\mathcal{L}_{μ} generates active powers (see (21)) but that globally \mathcal{L}_{μ} performs its inductance function in accordance with (22). By summing on "k" the 2 members of the first equation of (20) it comes:

$$P_{int} = P_{il}$$

(23)

III.3.2) Reactive powers. The second relations of (9) and (21) define, for $k > 1$, the equality:

$$Q''_{\mu k} = -(q_k + Q'_{\mu k}) \quad \text{for } k > 1$$

(24)

$i'_{\mu k}$ given by (10) allows to characterize $Q'_{\mu k}$: $Q'_{\mu k} = \hat{e}_k \hat{i}'_{\mu k} / 2$ with $Q'_{\mu k} = \hat{e}_k^2 / 2X'_{\mu k}$. It can be deduced that:

$$X'_{\mu k} = kX'_{\mu 1}$$

(25)

with:

$$X'_{\mu 1} = K_{MC}\omega / < \eta_r >$$

(26)

(25) therefore responds to a classical concept. Lines 8 and 42 of TA2 lead to: $X'_{\mu 1} = 7,747\Omega$.

Let us proceed, as for the active powers (see (22)), to the determination of:

$$- \sum_{k(k>1)} Q''_{\mu k} = \sum_{k(k>1)} (q_k + Q'_{\mu k})$$

(27)

The lines 43 and 44 of TA2 show that these sums are 0,636VAR that is much lower than $Q''_{\mu 1} = 22,112\text{VAR}$.

Let us introduce a quantity $Q''_{\mu 1(1)}$ such as:

$$Q''_{\mu 1} = Q''_{\mu 1(1)} - \sum Q''_{\mu k}$$

(28)

$Q''_{\mu(l)}$ defines a reactance $X''_{\mu(l)}$ attached exclusively to the fundamental. It means that $X''_{\mu(l)}$ does not contribute, like $X'_{\mu 1}$, through a quantity $kX''_{\mu(l)}$ to the definition of the quantities $i''_{\mu k}$ for $k>1$. The numerical applications show (Line 43) that $Q''_{\mu(l)} = 21,476\text{VAR}$ leading to associate with this quantity a reactance $X''_{\mu(l)}$ which is equal to $15,608\Omega$. It does not seem, a priori, obvious to define the analytical form of this reactance. As: $Q_{\text{int}} = Q_{\mu} = Q'_{\mu 1} + Q''_{\mu 1} + \sum_{k(k>1)} Q'_{\mu k} + \sum_{k(k>1)} Q''_{\mu k}$, it can be deduced that:

(29)

equality satisfied by considering the values of Q_{μ} (64,770VAR), of Q'_{μ} (43,294VAR) and that of $Q''_{\mu(l)}$ (21,476VAR) displayed at ligne 45.

$X_{\mu 1}$ relative to the fundamental associated to L_{μ} results from the parallel association of $X'_{\mu 1}$ and $X''_{\mu(l)}$. $X_{\mu 1}$ has consequently for value $5,177\Omega$. For $k>1$, the reactance to be considered is $X_{\mu k} = X'_{\mu k} = kX'_{\mu 1}$ with $X'_{\mu 1} = 7,747\Omega$.

III.3.3) Summary. These different relationships show that for sinusoidal v_G , the MC reacts according to a very specific concept which is stated as follows:

- i) The quantities $P_{\mu k}$ for $k>1$, generated by $P_{\mu 1}$, only serve to supply the necessary harmonic powers to independent elements of L_{μ} such as "r" and R_{ijk} .
- ii) The quantities $Q''_{\mu k}$ for $k>1$, generated by $Q''_{\mu 1}$, serve to provide the harmonic powers necessary for the elements kx independent of L_{μ} but also for elements of L_{μ} such that $kX'_{\mu 1}$.

The numerical values gathered in TA2 verify all the relations which have just been established. It is also possible to note that $i'_{\mu 1}$ and $i''_{\mu 1}$ both intervene significantly at the level of the definition of $i_{\mu 1}$. For $k>1$, it is $i''_{\mu k}$ which is largely preponderant compared to $i'_{\mu k}$ as to the definition of $i_{\mu k}$.

IV. CONSIDERATIONS ON THE EXPERIMENTAL DATA.

Given the stated objective, the original experimental data must undergo processing in order to be able to make credible comparisons with the results deduced from SAM referenced, in this case, SAM_{Exp} .

These experiments were carried out with a YOKOGAWA WT3000 precision wattmeter which makes it possible to carry out harmonic analyzes. The data are characterized by \hat{b}_{Ex} determined assuming "v" sinusoidal with $r_p=0$ and $x_p=0$.

12 statements relating to the following cases: 0,38T, 0,5T, 0,6T, 0,71T, 0,82T, 0,93T, 1,04T,

$$Q_{\text{int}} = Q_{\mu} = Q''_{\mu(l)} + Q'_{\mu}$$

1,15T, 1,26T, 1,37T, 1,47T, 1,55T were made. The corresponding data are grouped in DF.

IV.1) Data formatting.

- Practically, the original data characterizing the 3 external variables $v(t)$, $i(t)$ and $e(t)$ result from sequences of 1000 points on 2,5T ($\Delta t=0,05\text{ms}$) without knowing exactly what corresponds to the time origin. For given \hat{b}_{Ex} , this origin is common to all the signals recorded, however, nothing allows to conclude that this origin is preserved when \hat{b}_{Ex} pass to another value. The measuring device defines the average and rms values as well as the THDs of these signals. It also characterizes these signals by their FSs up to the hundredth rank (even and odd ranks) knowing that the time variables are affected by a signal of very low frequency and amplitude. Also displayed on the screen are the harmonic components of the active and reactive powers accessible for measurement as well as their overall values. As the original FSs show that the numerical values associated with the even ranks are all zero, the FSs of the variables and of powers are presented in DF by considering only the odd ranks up to rank 21. Also appear, for information, the quantities \hat{b}_k deduced from \hat{e}_k (see II.2.2).

- These different original sequences will first be rearranged. This rearranging has 3 phases.

- The first consists, for given \hat{b}_{Ex} , in extracting from the 3 sequences the data relating to T while ensuring, that for the initial instant, "v" presents a value close to its peak value. One out of two points is then eliminated, which leads to sequences which are defined on T with $\Delta t=0,1\text{ms}$.

- Then come the determinations of the FSs of the 3 rearranged variables.

- Finally, after having characterized FS(b), it is proceeded to the determination of b(t).

- In order to impose a common temporal origin on the different cases treated, these rearranged data have been reframed. As v_G is not accessible to measurement, the unique temporal origin adopted will merge with the instant which satisfies the condition $v_1 = \hat{v}_1$ at $t=0$, i.e. $v_1=0$. The principle

of this temporal reframing is based on the sequence redefinition of these signals from the FSs of the rearranged variables so that this reframing eliminates the low frequency component which affects the original data. DF gathers the coefficients of the FSs of the 4 reframed external variables as well as the associated powers.

- The comparison of the numerical values grouped together in DF makes it possible to appreciate the impact of the numerical manipulations leading to the final variable definitions. The original data actually undergoes slight modifications without significantly affecting the powers since the impact only relates to the last decimals. On the other hand, on THDs, given their definition, the impact is greater. For example, for $\hat{b}_{Ex}=1,55T$, \hat{b}_1 which originally had a value of 1,557T takes the value 1,553T with the reframed data. Regarding the THD on "e" it goes from 6,17% to 6,25%.

IV.2) First observations.

- The origin of these developments was to try to validate the presence of negative P_{int} and Q_{int} harmonic powers during various investigations carried out in order to rule out, in a categorical way, effects which could, perhaps, be linked to measurement errors. Note that these negative values led us to associate a "generator" function with L_{μ} . It would also have been possible to translate this behavior by introducing, at the level of harmonic powers, the notions of negative resistances and inductances as sometimes mentioned [24,25].

The information gathered in DF show that P_{int3} is negative for $\hat{b}_{Ex}=0,5T$. For $\hat{b}_{Ex}=1,15T$, these negative values concern P_{int3} and P_{int5} but also Q_{int3} . Then the number of terms concerned expands rapidly for $\hat{b}_{Ex}>1,15T$. This evolution is also accompanied by that of the modules of these quantities. Let us consider the original data. For $\hat{b}_{Ex}=1,26T$ for example, the relative difference between P_{int} and P_{int1} is -0,82%, it goes to -2,07% for $\hat{b}_{Ex}=1,37T$ until reach -42,47% for $\hat{b}_{Ex}=1,55T$. On this basis, it is, a priori, possible to attribute these "abnormalities" to saturation so that resorting to the notion of ESC for $\hat{b}_{Ex}<1,2T$ seems plausible.

In fact, for $k>1$, $\hat{e}_k \ll \hat{e}_1$. As a result, when \hat{b}_{Ex} decreases, the quantities P_{intk} and Q_{intk} for $k>1$ quite quickly take on very low values which, given the convention adopted to characterize the powers (3

decimals), are identified with "0". This means that the proposal made above concerning saturation must be accompanied by certain reservations.

- The experimental cases treated show differences in behaviors according to the values taken by \hat{b}_{Ex} . It is possible to analyze them by considering the active $i_{(a)}$ and reactive $i_{(r)}$ components of "i" that should be characterized beforehand. By definition, $i_{k(a)}$ is at the origin of the harmonic components of the active powers and $i_{k(r)}$ those of the reactive powers. At given "k", these components are defined with respect to the e_k . After having determined them for each value of "k", it suffices to define them in a common frame of reference which will be the reference frame ($v_1=0$) and add them to obtain $i_a(t)$ and $i_r(t)$ with: $i(t) = i_a(t) + i_r(t)$.

- $\forall \hat{b}_{Ex}$ it can be noted that $P_{int1}/Q_{int1} < 1$. This ratio is 0,15 for $\hat{b}_{Ex}=1,55T$, it goes to 0,72 for $\hat{b}_{Ex}=0,38T$. If for 1,55T the result is classic result ($\hat{i}_{l(a)}$ of the order of 10% of \hat{i}_l), this is no longer the case for 0,38T where $\hat{i}_{l(a)}$ and $\hat{i}_{l(r)}$ are practically of the same order of magnitude.

On the other hand, for $k=3$ for example, one can note that $P_{int3}/Q_{int3} > 1$. This ratio is 11 for 1,55T and 3,5 for 0,93T. This suggests that this ratio will approach 1 for 0,38T. If for $k=1$ the MC mostly exhibits behavior of an inductive nature, for $k>1$ this behavior, excluding considerations on the direction of power transfer, relate more to that of a receiver whose resistive and inductive elements are of the same order of magnitude.

These trends are justified by the operating equations presented knowing that for $k>1$: $P_{ilk} \ll p_k$. It follows that the proposition concerning the saturation formulated previously does not have to be. On the other hand, it suggests that the distortions on "i" will differ significantly depending on whether \hat{b}_{Ex} it is high or low.

- Considering the experimental data, Fig.4 presents, for $\hat{b}_{Ex}=1,55T$ and 0,38T, the following waveforms:

- Fig. 4a: variations of $i(t)$ for $\hat{b}_{Ex}=1,55T$ and 0,38T (multiplier coefficient of 30 on "i" for $\hat{b}_{Ex}=0,38T$),

- Fig. 4b: variations of $i_a(t)$ and $i_r(t)$ for $\hat{b}_{Ex}=1,55T$,

- Fig. 4c: variations of $i_a(t)$ and $i_r(t)$ for $\hat{b}_{Ex}=0,38T$.

On these figures also appears the reference $v_1(t)$, with an unspecified variable multiplier coefficient, since this variable has the sole interest of being able to position the different curves between them.

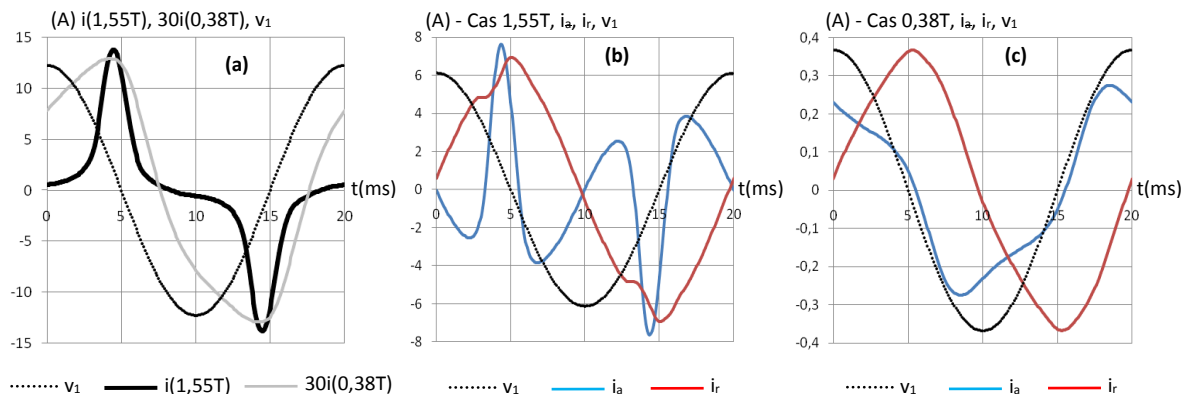


Fig. 4: Experimental variations of "i", ia and ir for $\hat{b}_{EX} = 1,55$ and $0,38T$

These plots validate the remarks made above. They also highlight a very particular point concerning the current peak on "i" for $\hat{b}_{EX} = 1,55T$. Simplistically, its justification results from a plot involving $b(t)$ and the curve $b(H)$ [1]. Implicitly, this assumes that this current peak is of a reactive nature whereas it is, on the whole, of an active nature as shown in Fig. 4b since essentially dependent on p_3 .

V. DETERMINATION OF THE ELEMENTS OF THE EQUIVALENT SCHEME.

V.1) Line components.

This determination uses the original data and more particularly:

- P_{extk} and Q_{extk} for $k > 1$ defined by (17) for r_G and x_G determinations,
- P_{intk} and Q_{intk} for $k > 1$ defined by (19) for "r" and "x" determinations and therefore those of r_p and x_p .

Fig. 5 presents, for the 12 experimental cases, the variations of r_G , $10x_G$, "r" and $10x$ as a function of \hat{b}_{EX} for k being successively 3 and 5. In accordance with what could be expected, it appears that the information which result from these investigations are all the more reliable as the numerical values of the quantities exploited are high. Implicitly, this means that k must limit itself to low values and \hat{b}_{EX} present high values.

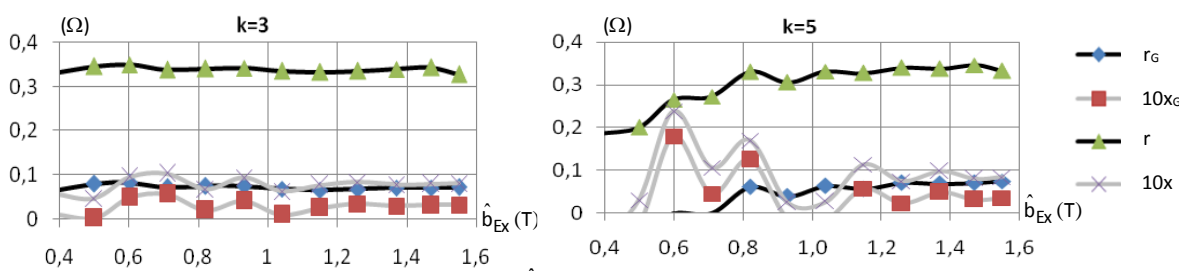


Fig. 5: Variations of r_G , $10x_G$, r and $10x$ as a function of \hat{b}_{EX} for the 12 experimental cases and for k being 3 and 5

Although the powers used are very low (for $\hat{b}_{EX} = 1,55T$, $|P_{ext3}|$ represents 3,5% of P_{ext1} and $|Q_{ext3}|$ a little less than 1% of Q_{ext1}), these original data lead for $k=3$ to fairly stable and similar values:

- concerning the resistances over the entire range of \hat{b}_{EX} variations,
- concerning the reactances for $\hat{b}_{EX} > 1T$.

For $k=5$ the powers considered are even lower, leading to increased fluctuations in the values of these elements. Nevertheless, a certain coherence characterizes them for $\hat{b}_{EX} > 1,2T$.

All of the measurements carried out led to the following values being retained: $r_G = 0,072\Omega$, $10x_G = 0,032\Omega$, $r = 0,341\Omega$, $10x = 0,083\Omega$ ie $r_p = 0,269\Omega$, $10x_p = 0,051\Omega$.

The reactances have very low values compared to the resistances (x_G 20 times lower than r_G). This ratio is accentuated concerning the quantities x_p and r_p , it goes to 160. This validates the conclusions formulated in II.1

concerning the short-circuit test which defined x_p as a quantity practically nul. r_p thus determined is slightly lower than the value deduced from the short-circuit test (0,31Ω).

It is interesting to note that, despite the presence of the power supply device (function generator associated with a power amplifier), the apparent upstream impedance of the "grid" which supplies the MC is characterized by quantities r_G and x_G which can, having regard to numerical inaccuracies, identify with constants. The other aspect concerns the hypothesis of a v_G supply with sinusoidal time evolution, whose origin is not identified, which from an experimental point of view may seem daring, which also seems justified.

This test campaign was relatively long so that the conditions under which the measurements were taken are not homogeneous (impact of temperature, users who connect or disconnect from the upstream grid, etc.). Nevertheless, it is possible to underline that elementary investigations on a saturated MC make it possible, independently of the notion of short-circuit power [26], to characterize the impedance of a grid. This particularity can prove to be very useful in the context of the design of certain devices [15].

V.2 Determination of the coefficients which characterize the iron loss components.

This determination, which also uses the original data, is based on the relation (23): $P_{int} = P_{il}$ which, in its formulation, is classic knowing that P_{int} is a variable accessible to measurement.

V.2.1) Principle implemented. Let us impose a model to characterize the fundamental iron losses by considering 3 components. Based on the scientific literature, these correspond to static (P_{ilSta1}), dynamic (P_{ilDyn1}) and excess (P_{ilExe1}) iron losses [27, 28]. This leads to defining P_{il1} by:

$$P_{il1} = K_{Sta} f \hat{b}_1^\xi + K_{Dyn} (f \hat{b}_1)^2 + K_{Exe} (f \hat{b}_1)^\varphi \quad (30)$$

with K_{Sta} , K_{Dyn} and K_{Exe} positive constants which, in principle, are independent of \hat{b}_1 . As specified in the literature φ takes the value 1,5 and ξ is assumed to be between 1,5 and 2,2. In practice, ξ will be assimilated to a parameter whose value will evolve from 1,3 to 2,3 with a step of 0,1.

Regarding the iron losses linked to \hat{b}_k , it is necessary to consider the P_{ilDynk} dynamic iron losses and those generated by the minor loops [29, 30]. As $\hat{b}_k \ll \hat{b}_1$ the latter will be neglected so that:

$$P_{ilk} = P_{ilDynk} = K_{Dyn} (k f \hat{b}_k)^2 \quad \text{for } k > 1 \quad (31)$$

It follows that the equation which governs the behavior of the MC in terms of P_{il} iron losses is written:

$$P_{il} = K_{Sta} f \hat{b}_1^\xi + K_{Exe} (f \hat{b}_1)^\varphi + K_{Dyn} f^2 \left[\hat{b}_1^2 + \sum_{k(k>1)} (k \hat{b}_k)^2 \right] \quad (32)$$

For a case of experiment \hat{b}_{Ex} , (32) reveals 3 unknowns which are K_{Sta} , K_{Exe} and K_{Dyn} . To identify them, it is necessary to consider a combination (Comb) made up of 3 distinct experimental cases among the 12 available. These cases will be distinguished using subscripts (o), (p) and (q). For case (o) for example, the values of $\hat{b}_{k(o)}$ are, $\forall k$, known. Hence the introduction, at given ξ , of the following known constants:

$$\left. \begin{aligned} A_{(o)} &= f \hat{b}_{1(o)}^\xi \\ B_{(o)} &= (f \hat{b}_{1(o)})^\varphi \\ C_{(o)} &= f^2 \left[\hat{b}_{1(o)}^2 + \sum_{k(k>1)} (k \hat{b}_{k(o)})^2 \right] \end{aligned} \right\} \quad (33)$$

It follows that for case (o), (32) is written:

$$P_{il(o)} = K_{Sta} A_{(o)} + K_{Exe} B_{(o)} + K_{Dyn} C_{(o)} \quad (34)$$

This Comb leads to a system of 3 equations with 3 unknowns. Its resolution makes it possible to distinguish, for all the values of ξ , those which lead to a possible solution. The acceptability criterion being that the 3 unknowns present, at given ξ , positive values.

Then another Comb of 3 cases is considered. Performing an analysis similar to the previous one leads to a new set of possible values of ξ .

Considering the 12 cases of experimentation, the number of possible Combs is quite large, hence a certain limitation in terms of the choices to be made. The final phase, by considering all the sets of possible values of ξ , consists in finding those which are common to all the Combs considered. One then proceeds to the choice of a value of ξ which leads to characterize K_{Sta} , K_{Dyn} and K_{Exe} .

The results obtained, presented in the form of tables, extracted from DF, are given below where the shaded boxes correspond to possible solutions.

V.2.2) Case of a model with 3 loss components.

The relations relating to this model are those which have just been presented. T1 groups certain results.

• Consider a Comb for which the MC is subjected to a pronounced saturation by identifying (o) to 1,55T, (p) to 1,47T and (q) to 1,37T. The numerical values obtained as a function of ξ are grouped together in T1.1 where also appear $P_{ill(o)}$, $P_{ill(p)}$ and $P_{ill(q)}$. T1.1 shows that no solution exists while the powers have consistent values. On the other hand, some numerical values are excessive (example of K_{Exe} and K_{Sta} for $\xi=1,5$).

• Assuming that (32) may not be applicable as such for states which correspond to relatively pronounced saturations, the Comb: (o)=0,6T, (p)=0,5T, (q)=0,38T was considered. The results obtained are grouped in T1.2. Again there is no solution with the same problem of excessive values

• The fact of modifying the value of φ but also of considering Combs involving more spaced \hat{b}_{Ex} values, did not make it possible to find a solution. Each time at least one of the unknowns presented a negative value except for $\varphi < 1,4$ without leading to a practical solution (common value of ξ valid simultaneously for several Combs). Hence the idea of falling back on a more rudimentary P_{il} model.

ξ	1,3	1,4	1,5	1,6	1,7	1,8	1,9	2	2,1	2,2	2,3
T1.1	(o)=1,55T - (p)=1,47T - (q)=1,37T..... $\varphi=1,5$										
K_{Dyn}	-0,0031	-0,0033	0,0014	-0,0038	-0,0041	-0,0045	-0,0048	-0,0053	-0,0058	-0,0064	-0,0072
K_{Exe}	0,1359	0,2461	1,2E+11	-0,1863	-0,0755	-0,0371	-0,0166	-0,0029	0,0076	0,0165	0,0249
K_{Sta}	-0,7502	-1,5181	8,4E+11	1,5671	0,7999	0,5464	0,4216	0,3487	0,3021	0,2709	0,2499
$P_{ill(o)}$	8,0968	8,1019	8,0010	8,1139	8,1210	8,1290	8,1381	8,1486	8,1607	8,1750	8,1920
$P_{ill(p)}$	7,3071	7,3084	7,2836	7,3113	7,3130	7,3149	7,3172	7,3197	7,3226	7,3261	7,3302
$P_{ill(q)}$	6,2221	6,2223	6,2185	6,2228	6,2231	6,2234	6,2237	6,2241	6,2246	6,2252	6,2258
T1.2	(o)=0,6T - (p)=0,5T - (q)=0,38T..... $\varphi=1,5$										
K_{Dyn}	-0,0003	-0,0005	0,0006	-0,0010	-0,0015	-0,0026	-0,0058	-26,4756	0,0070	0,0038	0,0027
K_{Exe}	0,0223	0,0382	1,8E+11	-0,0252	-0,0093	-0,0041	-0,0014	0,0039	0,0012	0,0020	0,0025
K_{Sta}	-0,0693	-0,1737	1,3E+12	0,3007	0,2153	0,2313	0,3726	1323,8514	-0,2866	-0,1319	-0,0826
$P_{ill(o)}$	1,6188	1,6188	1,6204	1,6188	1,6188	1,6188	1,6188	1,9788	1,6187	1,6187	1,6187
$P_{ill(p)}$	1,1843	1,1843	1,1846	1,1843	1,1843	1,1843	1,1843	1,3958	1,1842	1,1843	1,1843
$P_{ill(q)}$	0,7669	0,7669	0,7670	0,7669	0,7669	0,7669	0,7669	0,8686	0,7669	0,7669	0,7669

T1: 3 component model - Values of K_{Dyn} , K_{Sta} , K_{Exe} and P_{ill} as a function of ξ for 2 different Combs.

V.2.3) Case of a model with 2 loss components. This second model does not take excess losses into account. (32) which define P_{il} becomes:

$$P_{il} = K_{Sta} f \hat{b}_1^\xi + K_{Dyn} f^2 \left[\hat{b}_1^2 + \sum_{k(k>1)} (k \hat{b}_k)^2 \right] \tag{35}$$

In this case the equations that should be considered simultaneously are 2 in number. Therefore, a Comb will only have 2 experiment cases (o) and (p) with $P_{ill(o)}$ defined by:

$$P_{ill(o)} = K_{Sta} A_{(o)} + K_{Dyn} C_{(o)} \tag{36}$$

K_{Sta} and K_{Dyn} are always assumed to be positive constants independent of \hat{b}_1 . $A_{(o)}$ and $C_{(o)}$ are always defined by (33). ξ uses the same domain of variations as before. The Combs considered are: Comb(1): (o)=1,55T -

(p)=1,47T; Comb(2): (o)=1,47T - (p)=1,37T);.....;Comb(10): (o)=0,6T - (p)=0,5T; Comb(11): (o)=0,5T - (p)=0,38T.

These 11 Combs lead to solutions for different variation ranges of ξ . The only problem encountered concerns Comb(2) which does not present any intersection, in terms of ξ , with all the other combinations (Cf DF). Two ways can be considered to solve this problem:

- 1) consider that ξ can be variable,
- 2) group Comb(1) and Comb(2) leading to Comb(1,2): (o)=1,55T - (p)=1,37T.

By opting for the second solution, the values of K_{Dyn} , K_{Sta} , $P_{il(o)}$ and $P_{il(p)}$ as a function of ξ for $\varphi=1,5$ are grouped in T2 considering, for example, Comb(1,2) (T2.1), Comb(3) (T2.2), Comb(6) (T2.3) and Comb(11) (T2.4). It can be noted that over the range imposed for the possible variations of ξ , the number of boxes which lead to a solution seems to decrease when the Combs involve low values of \hat{b}_{Ex} . Nevertheless, there are 3 values of ξ which seem to meet the set objectives: $\xi=1,3$; 1,4; and 1,5.

\square	1,3	1,4	1,5	1,6	1,7	1,8	1,9	2	2,1	2,2	2,3
T2.1	Comb(1,2) : (o)=1,55T - (p)=1,37T..... $\varphi=1,5$										
K_{Dyn}	0,0013	0,0013	0,0013	0,0013	0,0013	0,0012	0,0012	0,0007	0,0016	0,0014	0,0014
K_{Sta}	0,0017	0,0019	0,0022	0,0026	0,0033	0,0045	0,0077	0,0335	-0,0129	-0,0052	-0,0031
$P_{il(o)}$	7,9961	7,9962	7,9964	7,9966	7,9969	7,9975	7,9990	8,0110	7,9893	7,9930	7,9939
$P_{il(p)}$	6,2182	6,2182	6,2182	6,2183	6,2183	6,2183	6,2183	6,2188	6,2180	6,2181	6,2181
T2.2	Comb(3) : (o)=1,37T - (p)=1,26T..... $\varphi=1,5$										
K_{Dyn}	0,0011	0,0010	0,0010	0,0009	0,0008	0,0005	-0,0003	-0,1175	0,0030	0,0022	0,0019
K_{Sta}	0,0146	0,0165	0,0193	0,0234	0,0304	0,0442	0,0854	5,9410	-0,0831	-0,0402	-0,0260
$P_{il(o)}$	6,2184	6,2185	6,2185	6,2186	6,2187	6,2190	6,2197	6,3245	6,2167	6,2174	6,2177
$P_{il(p)}$	5,3444	5,3444	5,3444	5,3444	5,3445	5,3446	5,3448	5,3802	5,3438	5,3441	5,3441
T2.3	Comb(6) : (o)=1,04T - (p)=0,93T..... $\varphi=1,5$										
K_{Dyn}	0,0006	0,0005	0,0003	-0,0000	-0,0005	-0,0015	-0,0044	-10,9322	0,0073	0,0044	0,0034
K_{Sta}	0,0414	0,0483	0,0580	0,0726	0,0970	0,1456	0,2915	546,6959	-0,2924	-0,1463	-0,0977
$P_{il(o)}$	3,8878	3,8878	3,8878	3,8879	3,8879	3,8880	3,8882	4,7879	3,8873	3,8875	3,8876
$P_{il(p)}$	3,2550	3,2550	3,2550	3,2550	3,2550	3,2551	3,2552	3,8340	3,2546	3,2548	3,2548
T2.4	Comb(11) : (o)=0,5T - (p)=0,38T..... $\varphi=1,5$										
K_{Dyn}	0,0010	0,0009	0,0007	0,0003	-0,0002	-0,0013	-0,0046	-70,7000	0,0086	0,0053	0,0042
K_{Sta}	0,0264	0,0334	0,0436	0,0592	0,0857	0,1395	0,3030	3535,1393	-0,3572	-0,1939	-0,1403
$P_{il(o)}$	1,1843	1,1843	1,1843	1,1843	1,1843	1,1843	1,1843	1,7492	1,1842	1,1842	1,1843
$P_{il(p)}$	0,7669	0,7669	0,7669	0,7669	0,7669	0,7669	0,7669	1,0385	0,7669	0,7669	0,7669

T2: - 2-component model - Values of K_{Dyn} , K_{Sta} and P_{il} as a function of ξ for different Combs.

For the rest of the analysis one will adopt for ξ the value of 1,4. This makes it possible not to consider a value of ξ which is at the level of a "solution-no solution" transition (like Comb(6) for example for $\xi=1,5$). Are grouped together in T3 the retained values of K_{Dyn} and K_{Sta} according to the Combs.

Comb	1,55-1,37	1,37-1,26	1,26-1,15	1,15-1,04	1,04-0,93	0,93-0,82	0,82-0,71	0,71-0,6	0,6-0,5	0,5-0,38
K_{Dyn}	0,0013	0,0010	0,0007	0,0005	0,0005	0,0005	0,0005	0,0006	0,0007	0,0009
K_{Sta}	0,0019	0,0165	0,0370	0,0456	0,0483	0,0478	0,0454	0,0420	0,0382	0,0334

T3: Selected values of K_{Dyn} and K_{Sta} as a function of Comb for $\xi=1,4$ and $\varphi=1,5$

In order to fix the orders of magnitude of the contribution of the different quantities, let us specify that for $\hat{b}_{Ex} = 1,55T$ the original data lead to $P_{int} = P_{il} = 8,026W$, $P_{int1} = 11,435W$. T2.1 shows that $P_{il} = 7,996W$ defining

$$\sum_{k(k>1)} P_{ilk} = 0,030W. \text{ As } \sum_{k(k>1)} p_k = 3,517W, (22) \text{ leads to } P''_{\mu l} = 3,547W. \text{ The relationship } P_{int1} = P_{il} + P''_{\mu l}$$

determines $P_{int1} = 11,543W$, i.e. a deviation of 0,94% from the measured value (11,435W). For this case, admit that $P_{int1} = P_{il}$ leads to an error of 43% on P_{il} . Fig. 6 shows the discontinuous variations of K_{Sta} and $10K_{Dyn}$ as a function of \hat{b}_{Ex} for the 10 Combs processed.

The first conclusion that can be formulated is that, contrary to what the analytical expressions of the iron loss components suggest, it is difficult to consider that K_{Sta} and K_{Dyn} can be identified with constants independent of

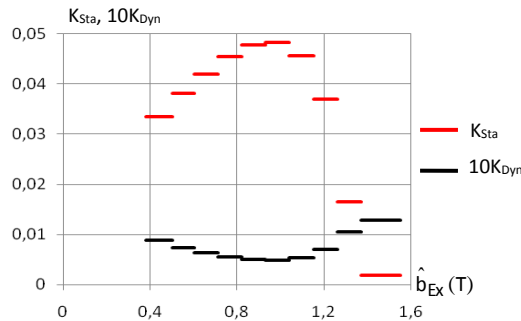


Fig. 6: Variations of K_{Sta} and $10K_{Dyn}$ with \hat{b}_{Ex}

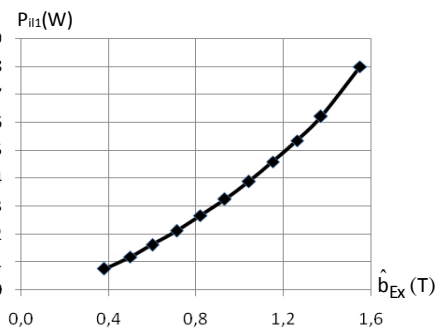


Fig. 7: Variations of P_{II1} with \hat{b}_{Ex}

\hat{b}_1 .

Examination of these different Combs shows, for given Comb, disregarding the values which correspond to $\xi=2$, that $P_{il(o)}$ and $P_{il(p)}$ are identified to constants independent of ξ . One can also note that the $P_{il(p)}$ of a Comb is identified with the $P_{il(o)}$ of the following Comb (in T2 this corresponds to the $P_{il(p)}$ of Comb(1,2) which is identified with the $P_{il(o)}$ of Comb(3)). This continuity on the powers leads to Fig. 7 which presents the variations of P_{II1} as a function of \hat{b}_{Ex} . There is a significant contrast between the variations of P_{II1} , which seem to conform to what one might expect, and those of K_{Sta} and K_{Dyn} .

V.2.4) Comments on the characterization of iron losses.

• First arises the problem of the exploitation of (32) which characterizes the iron losses using 3 components. It is about the impossibility of quantifying the coefficients K_{Sta} , K_{Dyn} and K_{Exe} even for \hat{b}_1 low values. It is stated in [31]: "the division of losses according to these 3 categories, although relatively arbitrary, is used by many authors". It therefore seems difficult to challenge (32) without providing adequate physical evidence. As this aspect is not the subject of this paper, the main reservation which can be formulated concerns the experiments. Many are those that make a distinction between these components using variable frequency tests implementing Epstein frame [32] or another dedicated device [21]. This way of proceeding places the "MC" in very specific conditions which are very different from those which characterize a magnetic device assembled to be, in practice, exploited. Indeed, in this case, the MC is affected by many constraints [33] which must significantly modify its behavior in terms of iron losses. Let us recall that if the metallurgists carry out these determinations of the iron losses by implementing a common device which is the Epstein frame, it is to be able to compare between them their products. Unfortunately, it would seem that in the context of industrial exploitation of these products, these data from metallurgists must be considered with reservations.

• The problem also concerns the 2 component loss model. If possible solutions appear, they must consider that the coefficients K_{Sta} and K_{Dyn} are functions of \hat{b}_1 . This particularity could, at the limit, be justified by taking into account a model to characterize the harmonic iron losses too rudimentary. However, the numerical application presented above shows that the P_{IIk} for $k>1$ are much too weak compared to P_{II1} to have an impact with such consequences.

• If one refers to the technical data of ArcelorMittal [34] for NO M400-50A, it is indicated: density 7,70kg/dm³, losses of 4W/kg for 1,5T peak. These data, which are similar to those announced by other producers of electrical steels (SIWAT, COGENT) lead, for the considered MC, to an estimate of P_{II1} which is of the order of 8,77W for $\hat{b}_1=1,5T$. Compared to our determination (8W for $\hat{b}_1=1,55T$), these manufacturer iron losses seem overestimated by around 9%. This difference is not negligible while being in contradiction with one of our previous remarks which evoked additional losses related to the assembly problem. Apart from any other consideration, this overestimation of losses by the manufacturer is all the more surprising since, from a competitive point of view, the tendency would rather be to underestimate losses.

V.2.5) Considerations on Epstein frame.

The numerical application presented in V.2.3 shows that the P_{IIk} for $k>1$ are negligible compared to the

p_k , $P_{\mu k}$ will be, $\forall k$, mainly dependent on p_k . The fact of being able to neglect the P_{ilk} makes it possible to consider that "b" is sinusoidal what leads to draw a parallel with Epstein frame at the level of which a servo-control theoretically imposes this waveform on "b". Let us assume that this control allows to strictly satisfy the equality $e=e_1$. This supposes that this control disturbs "v" (see Fig. 3) by generating harmonics which must satisfy the equalities: $v_k - u_{pk}=0 \forall k>1$. If this is the case, it means more particularly that the p_k for $k>1$ are all provided by "v". As the e_k for $k>1$ are zero, the P_{ilk} for $k>1$ are also zero. It follows that $P_{\mu k}=0$ for $k>1$ and therefore that $P_{\mu 1}=0$ leading to: $P_{int}=P_{int1}=P_{i11}$. In practice, the finesse with which is defined "b" is rarely communicated so that the equalities between v_k and $u_{pk} \forall k>1$ in the strict sense are probably not satisfied by any device, however sophisticated, for try to satisfy this condition [9]. If this aspect has negligible consequences on the P_{ilk} for $k>1$, it is not the same for the p_k ($k>1$) of which only a part will be provided by the v_k knowing that the remaining part will be generated by the MC according to the developed theory. It follows that $P_{\mu 1} \neq 0$ leading to polluting P_{int1} and therefore to overestimate P_{i11} . This aspect justifies the last observation made in V.2.4 which specifies that the manufacturer's data probably overestimates the fundamental iron losses.

V.3) Determination of the R_{ilk} .

	Comb(1,2) : (o)=1,55T; (p)=1,37T		Comb(3) : (o)=1,37T; (p)=1,26T		Comb(6) : (o)=1,04T; (p)=0,93T		Comb(11) : (o)=0,5T; (p)=0,38T	
	(o)	(p)	(o)	(p)	(o)	(p)	(o)	(p)
R_{i1Sta} (Ω)	1681,625	1558,604	180,108	171,579	52,337	48,962	48,611	41,572
R_{i1Dyn} (Ω)	38,153	38,153	46,947	46,947	101,954	101,954	56,131	56,131
R_{i11} (Ω)	37,307	37,241	37,240	36,861	34,584	33,077	26,050	23,883

T4: Characterization of R_{i1Sta} , R_{i1Dyn} and R_{i11} (for $k>1 R_{ilk}=R_{i1Dyn}$) for different combinations, $\xi=1,4$ and $\phi=1,5$

- The analysis of the R_{i11} values makes it possible to verify, as for P_{i11} previously, that, considering numerical errors, the $R_{i11(p)}$ of one combination is identified with the $R_{i11(o)}$ of the following one. In T4 this corresponds to $R_{i11(p)}$ of Comb(1,2) which is identified with $R_{i11(o)}$ of Comb(3). $R_{i11}(\hat{b}_{Ex})$ therefore appears as a single continuous curve.
- The R_{i1Dyn} are characterized by a discontinuous function consisting of a succession of segments of the type presented in Fig. 6. This means that the value of R_{i1Dyn} for Comb(n) do not correspond to the experiment values relative to $\hat{b}_{Ex(o)}$ and $\hat{b}_{Ex(p)}$. Hence the hypothesis of considering that over the interval Comb(n), R_{i1Dyn} evolves linearly from M to N as presented in Fig. 9 with:

$$R_{i1DynComb(n)M} = \left[R_{i1DynComb(n-1)} + R_{i1DynComb(n)} \right] / 2$$

$$R_{i1DynComb(n)N} = \left[R_{i1DynComb(n)} + R_{i1DynComb(n+1)} \right] / 2 \quad (37)$$

Consider a Comb relative to $\hat{b}_{Ex(o)}$ and $\hat{b}_{Ex(p)}$. For each of these values of \hat{b}_{Ex} one retrieves the FSs of the reframed data. As K_{Dyn} and K_{Sta} are known, one proceeds, according to the values of "k", to the determinations of the P_{ilk} . As: $P_{ilk} = \hat{e}_k^2 / 2R_{ilk}$, the R_{ilk} values relative to $\hat{b}_{Ex(o)}$ and $\hat{b}_{Ex(p)}$ can be deduced.

R_{i11} results from 2 effects: static and dynamic losses. R_{i11} is therefore made up of the parallel association of R_{i1Sta1} and R_{i1Dyn1} . For $k>1$, R_{ilk} only takes dynamic effects into account: $R_{ilk}=R_{i1Dynk}$.

The dynamic iron losses are, $\forall k$, given by (31). As:

$$P_{i1Dynk} = \hat{e}_k^2 / 2R_{i1Dynk}, \text{ the } \hat{b}_k \text{ expression (see II.2.2)}$$

leads to: $R_{i1Dynk} = 2(nS_{MC}\pi)^2 / K_{Dyn}$. As a result, at a given Comb, the R_{i1Dynk} identify themselves with a constant $\forall k$. Therefore, the quantities R_{i1Dynk} will simply be noted R_{i1Dyn} . Are grouped in T4 the values obtained from R_{i1Sta} , R_{i1Dyn} and R_{i11} for the 4 combinations which appear in T2 knowing that R_{ilk} for $k>1$ identifies with R_{i1Dyn} .

Fig. 8 shows the variations of these resistances as a function of \hat{b}_{Ex} . For R_{i1Sta} and R_{i1Dyn} , instead of representing them using segments as in Fig. 6, the high and low envelope curves appear as well as the average characteristics.

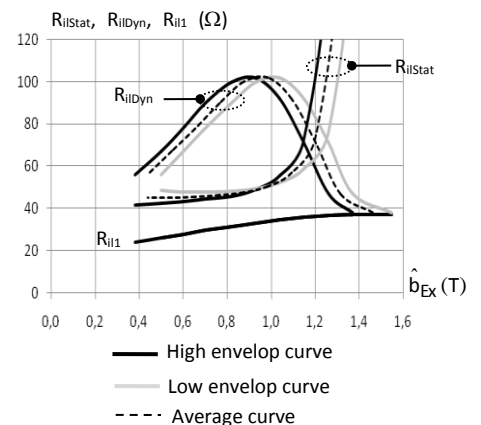


Fig. 8: Variations of R_{i1Stat} , R_{i1Dyn} and R_{i11} with \hat{b}_{Ex}

With this method, it is not possible to define the quantities given by (37) for Comb(1,2) and Comb(11). To remedy this, it suffices to introduce 2 fictitious Combs referenced Comb(0) and Comb(12) obtained by extrapolation of the data which appear in T4. Those Combs that complete T4 appear in T5.

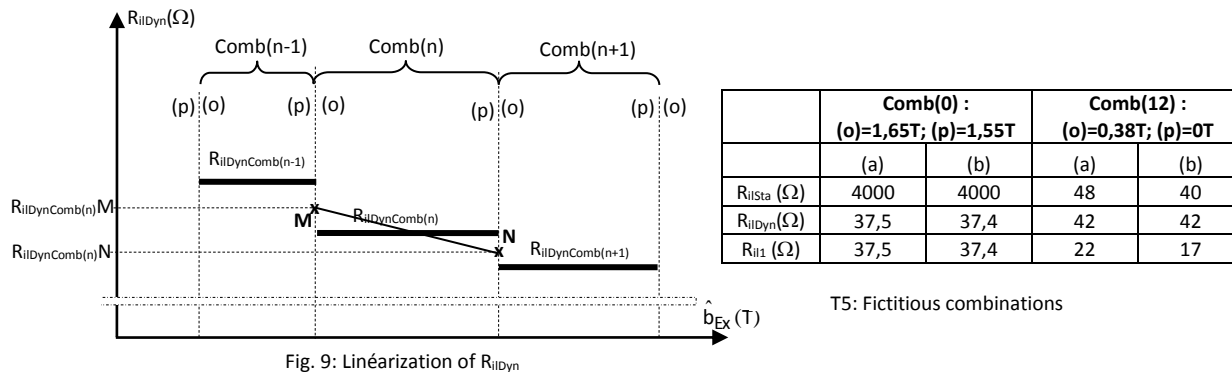


Fig. 9: Linéarization of R_{iiDyn}

• The interest of this characterization is to be able to predetermine $i_{il}(t)$. To overcome the peculiarity of R_{iiSta} , the following expression of i_{il} is considered:

$$i_{il} = \frac{e_1}{R_{ii1}} + \frac{(e - e_1)}{R_{iiDyn}} \quad (38)$$

The values of R_{iiDyn} and R_{ii1} relating to the 12 experimental cases are presented in T6, knowing that the values of these quantities for $\hat{b}_{Ex} = 1,47T$ result from those of $\hat{b}_{Ex} = 1,55T$ and $\hat{b}_{Ex} = 1,37T$ by considering linear variations of R_{ii1} and R_{iiDyn} over the interval relating to Comb(1,2). It should be kept in mind that the R_{iiDyn} values for $\hat{b}_{Ex} = 1,55T$ and $0,38T$ are given with some uncertainty due to how they were determined. The variations of R_{iiDyn} and R_{ii1} as a function of \hat{b}_{Ex} are not represented because these are very close to those given in Fig. 8 considering the average curve for R_{iiDyn} .

\hat{b}_{Ex} (T)	1,55	1,47	1,37	1,26	1,15	1,04	0,93	0,82	0,71	0,6	0,5	0,38
R _{iiDyn} (Ω)	37,826	39,926	42,550	58,976	81,501	96,975	100,914	94,880	83,968	72,603	61,644	49,065
R _{ii1} (Ω)	37,307	37,278	37,241	36,860	35,908	34,584	33,077	31,435	29,711	27,894	26,050	23,883

T6: Values of R_{iiDyn} and R_{ii1} for the 12 experimental cases

• Fig. 8 shows that R_{iiSta} exhibits significant effects up to around 1,2T, i.e. for operations not too affected by saturation. For $\hat{b}_{Ex} > 1,2T$, the role of R_{iiSta} in terms of losses becomes secondary and very quickly becomes insignificant. Consequently, in a saturated regime, the P_{il} are dependent only on the dynamic effects with $R_{ii1} \approx R_{iiDyn}$ and values which stabilize when the saturation increases.

R_{iiSta} variations are more complex. Indeed, T4 shows that R_{iiSta} varies over the interval corresponding to a Comb and displays a discontinuity when passing from one Comb to another.

• Concerning the problem encountered with Comb(2) for the determinations of K_{Sta} and K_{Dyn} , Fig. 8 shows that it is around 1,4T that K_{Sta} begins to take particularly high values which are, perhaps, at the origin of this difficulty.

• Conventional tests using the ESC notion (see II) lead to R_{ii1} of 31,8Ω for \hat{b} the order of Tesla.

Considering T4, a slightly higher value of 34,6Ω for 1,04T is obtained.

• The essential particularity relates to the R_{iik} which are not identified with constants. One possibility concerns the formulation of these losses which must probably be more complex than the expressions proposed in the literature. We do not think that this aspect has already been mentioned or if this reverse procedure with identification which has been exploited has already been used. As the objectives of this paper are not centered on this specific aspect, will be considered later, at given \hat{b}_{Ex} , the constants which appear T6.

V.4) Definition of the characteristic $\mu_r(b)_{Exp}$.

The objective is to define a single characteristic $\mu_r(b)_{Exp}$ relating to the magnetic material, valid whatever the value taken by "b" over the interval [0T-1,65T], from the partial characteristics determined for the different values of \hat{b}_{Ex}

V.4.1) Explanation of the procedure. This exploits the time data of the reframed signals ($v_1=0$). Practically, the characteristic $\mu_r(b)$ presents a symmetry with respect to the ordinate axis so that for this determination, it suffices to limit the investigations to a time interval of 5ms knowing that the instant "t" which leads to \hat{b} is close, by lower values, to 5ms. For given \hat{b}_{EX} , (38) defines $i_{il}(t)$ which leads to $i_{\mu}(t)$: $i_{\mu}(t) = i(t) - i_{il}(t)$. Taking $b(t)$ into account allows, in accordance with (3), to define $\mu_r(t)$. This way of proceeding to determine $\mu_r(\hat{b}_{EX})$ presents a certain number of problems like those generated by the passages by 0 of i_{μ} . Moreover, even in the vicinity of \hat{b}_{μ} , there are significant uncertainties. To illustrate them, the

- determine the characteristics $\mu_r(\hat{b}_{EX})$ according to the methodology presented,
- retain for each case the coordinates of the point which leads to the maximum values of μ_r and "b" (points marked by "x" in Fig.10 and for which the considered values of the R_{ilk} have a physical meaning since resulting from a theoretical approach). This leads to 12 points, grouped in T7, which define the characteristic $\mu_r(b)_{EXP}$ of

characteristics $\mu_r(\hat{b}_{EX})$ for $\hat{b}_{EX}=1,37T$ and $1,26T$ are plotted in Fig. 10a with a zoom of these characteristics in the vicinity of the \hat{b} values in Fig. 10b. Although the \hat{b}_{EX} values are quite close, there are significant differences between these characteristics for low values of "b". A gap appears also on the zoom which will be all the more pronounced as the difference between the \hat{b}_{EX} values will be significant. It is possible to consider using the manufacturer's data for these determinations. However the catalogs do not present a sufficiently rich panel in terms of $b(H)$ characteristics in order to be able to trace sufficiently accurately the complete $\mu_r(b)_{EXP}$. As our experiments fill this gap, the procedure used will be the following:

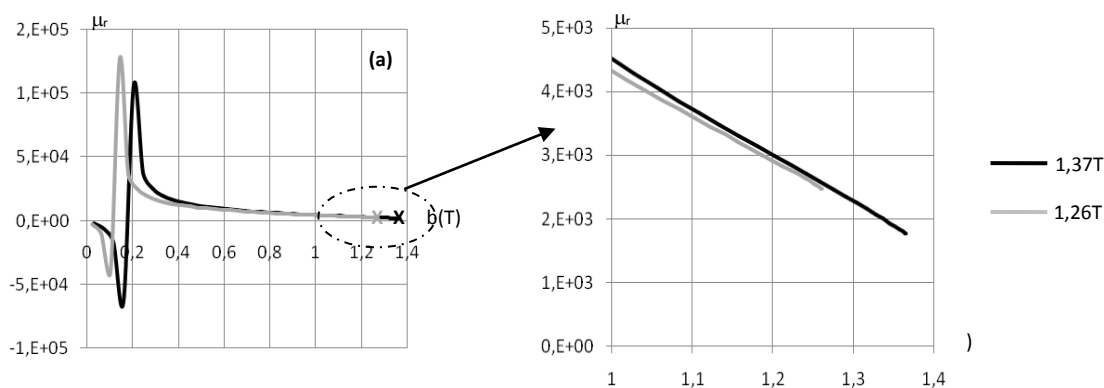


Fig. 10: Characteristics $\mu_r(\hat{b}_{EX})$ for $\hat{b}_{EX}=1,37T$ and $1,26T$: (a) Complete, (b) Zoom in the vicinity of \hat{b}

Fig. 11.

b_{max}	0,385	0,499	0,604	0,714	0,823	0,932	1,042	1,153	1,261	1,365	1,471	1,542
μ_{rmax}	4206,9	4444,0	4455,8	4328,8	4100,0	3808,7	3455,2	3014,6	2474,4	1766,2	910,8	507,8

T7: Points of the $\mu_r(\hat{b}_{EX})$ characteristics deduced from the experimental data.

It is interesting to note that the area marked with a circle in Fig. 11, shows a change in concavity of $\mu_r(b)_{EXP}$ which occurs around $1,47T$. The question arises of the possible link between this inflection point and the rapid increase in K_{Sta} in this area. On the other hand, this change of concavity announces that $\mu_r(b)_{EXP}$, for higher flux densities, will merge with a straight line which will present a slightly negative slope admitting the abscissa axis as an asymptote.

This way of proceeding is relatively conventional implementing, in fact, the characteristics $b(i)$. It is justified for states for which \hat{b} is not very high because the hypothesis which consists in considering that at time "t", which leads to \hat{b} , $i_{il}=0$ and therefore that $i=i_{\mu}$ with $i_{\mu}=\hat{i}_{\mu}$, is probably justified. For high \hat{b} this is not the case because i_{μ} includes an active component so that \hat{b} and \hat{i}_{μ} do not appear at the same instants. To test the validity of the proposed procedure, Fig. 12 presents cycles $b(i)$ and $b(i_{\mu})$ for $\hat{b}_{EX}=1,04T$. As the area of a cycle is representative of the P_{il} , the passing of $b(i)$ to $b(i_{\mu})$, shows that this area is considerably reduced. Nevertheless it appears that i_{μ}

is perturbed by a small harmonic component of order 3. It is however possible to conclude, even if the result is not perfect, that one comes very close to the anhysteretic curve and therefore that the determination of i_μ , given the complexity of the procedure used to identify the R_{ilk} , seems consistent.

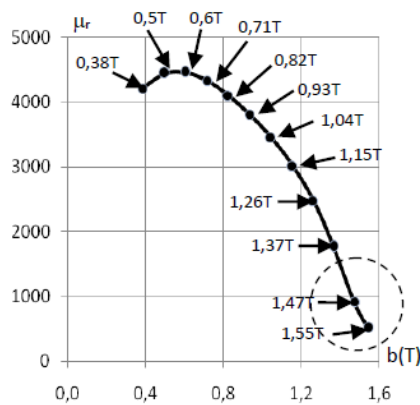


Fig. 11: $\mu_r(b)_{Exp}$ Characteristic

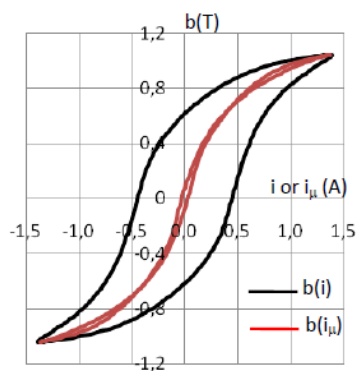


Fig. 12: Cycles $b(i)$ and $b(i_\mu)$ for $\hat{b}_{Ex} = 1,04T$

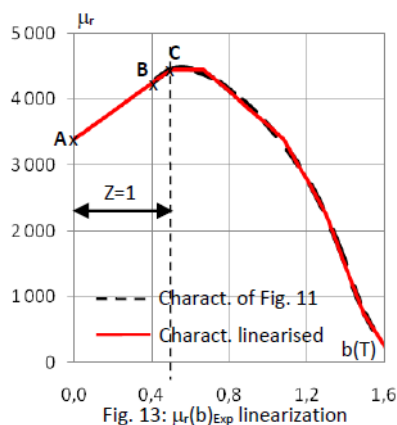


Fig. 13: $\mu_r(b)_{Exp}$ linearization

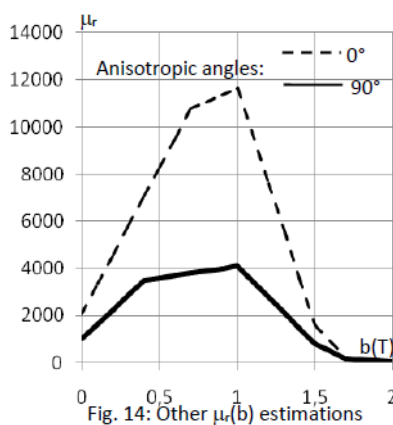


Fig. 14: Other $\mu_r(b)$ estimations

Z↓	$\mu_{r,(Z-1)}$	$\mu_{r,(Z)}$	$b_{lim,(Z-1)}$	$b_{lim,(Z)}$	α_z	β_z
1	3400	4450	0	0,5	3400,0	2100,0
2	4450	4450	0,5	0,67	4450,0	0,0
3	4450	3400	0,67	1,08	6165,9	-2561,0
4	3400	2250	1,08	1,3	9045,5	-5227,3
5	2250	750	1,3	1,49	12513,2	-7894,7
6	750	50	1,49	1,65	7268,8	-4375,0

T8: Characterization of segments of linearized $\mu_r(b)_{Exp}$

V.4.2) Linearization of the characteristic $\mu_r(b)_{Exp}$.

Fig. 13 presents the linearized characteristic according to 6 segments of $\mu_r(b)_{Exp}$. The lack of information on the interval [0T - 0,38T] led us to simply extrapolate in this zone the characteristic presented in Fig. 13 while keeping the leading coefficient of section CB [0,385T - 0,499T]. Hence the segment AB of Fig. 13 which, with BC, define the segment AC relative to $Z=1$. T8 presents the data that characterizes these different segments.

For comparison, Fig. 14 presents the 5-segment linearized $\mu_r(b)$ characteristics of the NO M400-50A estimated from other methods for 0° [13] and 90° anisotropic angles. As no precaution was taken as for the assembly of the stack of sheets of the considered MC [35, 36], it was possible to expect that $\mu_r(b)_{Exp}$ of the MC is located approximately equidistant from the 2 extreme characteristics of Fig. 14. It appears that this is not the case since $\mu_r(b)_{Exp}$ is close to the characteristic relating to the 90° anisotropic angle of Fig. 14. This rather

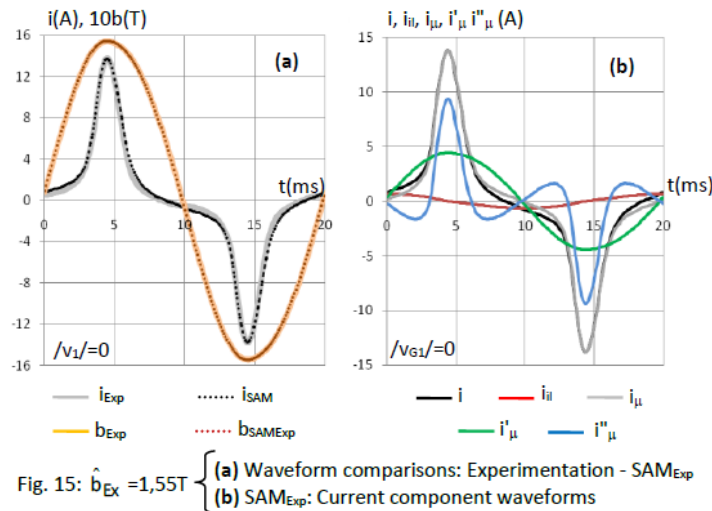
particular position is probably justified by the uncertainties linked to the MC assembly procedure

VI. "EXPERIMENTATION - SAM_{Exp}" COMPARISON for $\hat{b}_{Ex}=1,55T$.

This comparison consists in implementing SAM by integrating as input data the elements determined in paragraph 5. Under these conditions, SAM is referenced SAM_{Exp}. Comparison of the results thus obtained with those deduced from experimental measurements will make it possible to validate or not the developments presented in this article. This analysis will only concern the case $\hat{b}_{Ex}=1,55T$ taking as reference the \hat{b}_1 experimental value. V_{G1} will be adjusted so that \hat{b}_1 given by SAM_{Exp} identifies with this reference. The

[33].

comparison concerns $i(t)$ and $b(t)$. It presents a problem because the experimental variables are defined with a temporal origin characterized by $/v_1/=0$ whereas the implementation of SAM_{Exp} considers an origin relative to $/v_{G1}/=0$. To get rid of this problem, it suffices to proceed to a temporal change of the variables resulting from SAM_{Exp} in order to redefine them with a temporal origin linked to $/v_1/=0$. Fig. 15a presents these variables for the 2 cases for $/v_1/=0$. Fig. 15b presents the variations on T of "i", i_{il} , i_{μ} , i'_{μ} and i''_{μ} deduced from SAM_{Exp} for $/v_{G1}/=0$. The main numerical values relating to these behaviors are grouped in T9.



The comparison of the "i" waveforms (Fig. 15a) seems particularly convincing of the validity of our model. There is an appreciable difference on the currents for low values of "b" ($|b|<0,4T$) which is essentially dependent on the inaccuracy resulting from the lack of information on the definition of $\mu_r(b)_{Exp}$ in this area. This also results in some small differences which affect the powers (see T9) which specifies that $i_{\mu 1(a)}$ intervenes for 28,8% in the definition of $i_{1(a)}$ (this percentage also defining the impact of $P_{\mu 1}$ on P_{int1}).

As our objectives are to be able to characterize an MC subjected to high saturations, the results presented conclude that the goal is achieved. In addition, this comparison validates the theoretical model proposed as well as the procedures used to identify the elements of the equivalent scheme.

For values of $\hat{b}_{Ex}<1,55T$ the differences between the experimental waveforms and those deduced from SAM_{Exp} are a little more marked and this all the more so as \hat{b}_{Ex} moves away from 1,55T. This is justified by the fact that the contribution of $|b|<0,38T$ (which seems to pose a problem) at the level of the definition of the signals using SAM_{Exp} becomes, at the scale of T, more and more impacting. This aspect is all the more constraining in view of the fact that the behavior of the MC for low values of "b" is quite specific as shown by the analysis presented in IV.2 but also taking into account [37]. Implicitly this means that the simple extrapolation carried out in the area of low values of "b" does not seem appropriate.

VII. CONCLUSION

The developments presented define the complete system of equations which governs, in steady state under presumed sinusoidal voltage, the behavior of a single-phase MC by taking into account the non-linearities of its magnetic material. The first particularity linked to these specific equations is that they translate the behavior of this MC on the basis of its conventional equivalent scheme. On the other hand, these equations make it possible to identify all the components of this scheme which, for some of them, present rather singular behaviors. The last point, not the least, concerns the characterization, in terms of impedance, of the grid which supplies this MC leading, more generally, to the definition of a procedure which makes it possible to identify any grid by simply exploiting a transformer operating at no-load in saturated mode.

The comparison of the experimental results with those deduced from SAM for the case of an MC subjected to an important saturation, makes it possible to appreciate the relevance and the reliability of these various identifications and thus of the validity of the system of equations presented. This analysis also reveals a problem

related to the low values of "b". This aspect which, a priori, may surprise, deserves a more in-depth analysis.

Although this is not the primary concern of these investigations, it has been shown that the determination of fundamental iron losses using an Epstein frame (or other dedicated devices) could be tainted with significant errors. The salient point related to this observation is dependent on the very cause of these errors which does not seem to have already been mentioned in the scientific literature and which deserves very special attention. We propose, in the context of a future paper, to suggest a methodology, based on the existing concept in terms of structure, which makes the results obtained more reliable.

If this article provides answers to certain questions, it opens new perspectives to try to respond to certain behaviors that have emerged during the presentation of these developments. Answering some of them will no doubt make it possible to better understand the behavior of this elementary MC and, why not, to highlight specific behaviors that could be the source of new concrete applications.

Line ↓	D) EXPERIMENTATION - reframed data for $\hat{b}_{Ex} = 1,55T$ - Temporal reference: $v_i=0$													
1	I.1) FSS of external variables													
2	k	1	3	5	7	9	11	13	15	17	19	21	rms	THD(%)
3	$v_k(V)$	24,69 3	0,294	0,159	0,094	0,037	0,018	0,019	0,018	0,016	0,016	0,014	17,46 2	1,42
4	$/v_k(^{\circ})$	0,00	52,33	213,1 0	8,66	154,8 0	-	76,90	36,20	175,4 5	149,0 0	-	44,79	
5	$i_k(A)$	6,303	3,793	2,146	1,099	0,437	0,135	0,067	0,055	0,032	0,016	0,015	5,484	58,26
6	$/i_k(^{\circ})$	77,73	244,1 2	45,11	207,6 7	3,06	137,7 3	228,0 1	-1,50	135,6 2	256,4 5	20,79		
7	$e_k(V)$	24,37 1	1,274	0,722	0,389	0,159	0,059	0,036	0,031	0,023	0,017	0,013	17,26 6	6,25
8	$/e_k(^{\circ})$	-3,70	58,91	218,2 6	17,23	169,0 7	-	57,14	40,70	172,7 5	-	127,5 4	59,12	
9	$b_k(T)$	1,553	0,027	0,009	0,004	0,001	0,000	0,000	0,000	0,000	0,000	0,000		1,86
10	$/b_k(^{\circ})$	86,30	148,9 1	-	107,2 3	259,0 7	-	32,86	130,7 0	262,7 5	-	217,5 4	30,88	
11	I.2) Powers relative to external variables													Σk
12	$P_{extk}(W)$	16,54 0	-	-	-	-	-	-	-	-	-	-	15,76 9	
13	$Q_{extk}(VAR)$	76,04 0	-	-	-	-	-	-	-	-	-	-	75,86 9	
14	$P_{intk}(W)$	11,44 4	-	-	-	-	-	-	-	-	-	-	8,018	
15	$Q_{intk}(VAR)$	75,94 5	-	-	-	-	-	-	-	-	-	-	75,58 5	
16	II) SAM _{Exp} - Characterization of external variables - Temporal reference: $v_i=0$													
17	Parameters: $r=0,341\Omega$, $x=0,0083\Omega$, $r_p=0,269\Omega$, $x_p=0,0051\Omega$, $R_{ill}=37,307\Omega$, $R_{illvni}=37,826\Omega$.													
18	II.1) Operating conditions: $V_{G1}=17,567V$ - Tests on V_{Gth} : $THD(V_{Gth})=1,12*10^{-6}\%$, $\delta V_{Gth1}^{\wedge}=1,76*10^{-8}V$, $\delta/V_{Gth1}=-4,11*10^{-7}$													
19	II.2) FSS of external variables													
20	k	1	3	5	7	9	11	13	15	17	19	21	rms	THD(%)

21	$v_k^{\wedge}(V)$	24,71 7	0,266	0,151	0,072	0,029	0,010	0,007	0,006	0,003	0,001	0,002	17,47 9	1,28
22	$/v_k^{\wedge}(^{\circ})$	0,00	59,29	215,3 4	6,72	152,0 2	260,7 3	1,60	138,8 7	280,1 7	- 42,56	56,96		
23	$i_k^{\wedge}(A)$	6,770	3,662	2,045	0,958	0,376	0,129	0,080	0,069	0,030	0,009	0,024	5,679	53,81
24	$/i_k^{\wedge}(^{\circ})$	78,04	246,8 8	47,82	203,8 7	-6,44	106,3 4	210,9 3	-8,42	135,9 3	175,9 3	277,8 9		
25	$e_k^{\wedge}(V)$	24,37 0	1,252	0,702	0,331	0,131	0,046	0,029	0,025	0,011	0,003	0,009	17,26 4	6,06
26	$/e_k^{\wedge}(^{\circ})$	-4,18	62,71	220,9 1	14,28	161,3 6	271,6 3	13,83	152,2 1	- 65,60	- 27,60	72,49		
27	$b_k^{\wedge}(T)$	1,553	0,027	0,009	0,003	0,001	0,000	0,000	0,000	0,000	0,000	0,000		1,82
28	$/b_k^{\wedge}(^{\circ})$	85,82	152,7 1	- 49,09	104,2 8	251,3 6	1,63	103,8 3	242,2 1	24,40	62,40	162,4 9		
29		II.3) Powers relative to external variables											Σk	
30	$P_{extk}(W)$	17,34 1	- 0,483	- 0,151	- 0,033	- 0,005	- 0,001	0,000	0,000	0,000	0,000	0,000	16,66 8	
31	$Q_{extk}(VAR)$	81,84 6	- 0,064	- 0,033	- 0,010	- 0,002	- 0,000	0,000	0,000	0,000	0,000	0,000	81,73 5	
32	$P_{intk}(W)$	11,17 7	- 2,287	- 0,713	- 0,157	- 0,024	- 0,003	- 0,001	- 0,001	0,000	0,000	0,000	7,992	
33	$Q_{intk}(VAR)$	81,72 9	- 0,167	- 0,086	- 0,026	- 0,005	- 0,001	0,000	0,000	0,000	0,000	0,000	81,44 3	
34		III) SAM_{Exp} - Characterization of internal variables - Temporal reference: $/v_{G1}/=0$ ($/v_1/=-1,09^{\circ}$)												
35		III.1) "Losses"											Σk	
36	$p_k(W)$	7,814	2,287	0,713	0,157	0,024	0,003	0,001	0,001	0,000	0,000	0,000	10,99 9	
37	$q_k(VAR)$	0,190	0,167	0,086	0,026	0,005	0,001	0,000	0,000	0,000	0,000	0,000	0,476	
38	$P_{ilk}(W)$	7,960	0,021	0,007	0,001	0,000	0,000	0,000	0,000	0,000	0,000	0,000	7,989	
39		III.2) Powers relative to internal variables ($P'_{\mu k}=0$)											Σk	
40	$P_{\mu k}=P'_{\mu k}(W)$	3,217	- 2,307	- 0,720	- 0,158	- 0,024	- 0,003	- 0,001	- 0,001	0,000	0,000	0,000	0,003	
41	$p_k+P_{ilk}(W)$	15,77 4	2,307	0,720	0,158	0,024	0,003	0,001	0,001	0,000	0,000	0,000	18,98 8	
42	$Q_{\mu k}(VAR)$	81,72 9	- 0,167	- 0,086	- 0,026	- 0,005	- 0,001	0,000	0,000	0,000	0,000	0,000	81,44 3	
43	$Q'_{\mu k}(VAR)$	54,12 3	0,048	0,009	0,001	0,000	0,000	0,000	0,000	0,000	0,000	0,000	54,18 2	
44	$Q''_{\mu k}(VAR)$	27,60 6	- 0,214	- 0,095	- 0,028	- 0,005	- 0,001	0,000	0,000	0,000	0,000	0,000	27,26 1	
45	$q_k+Q'_{\mu k}(VAR)$	54,31 4	0,214	0,095	0,028	0,005	0,001	0,000	0,000	0,000	0,000	0,000	54,65 8	
46		III.3) Reactances relative to the fundamental (pour $k>1$ $:X_{\mu k}=kX'_{\mu 1}$)						III.4) Proportion $i_{\mu 1(a)}/i_{1(a)}$						
47		$X'_{\mu 1}=5,487\Omega$		$X''_{\mu 1(1)}=10,893\Omega$		$X_{\mu 1}=3,649\Omega$		$i_{\mu 1(a)}/i_{1(a)}=28,78\%$						

T9: Numerical data deduced from experimentation and from SAM_{Exp} for $\hat{b}_{EX}=1,55T$ ($\hat{b}_1=1,553T$)

For convenience \hat{y}_k in T9 is denoted y_k^{\wedge}

APPENDIX A: SAM PRESENTATION - ANALYSIS OF A THEORETICAL CASE

A1) Principle of the method.

This method assumes knowing the line and magnetic block components (R_{ilk} quantities and $\mu_r(b)$ characteristic) as well as the input variable v_G which is identified with v_{G1} : $v_{G1} : v_{G1} = \hat{v}_{G1} \cos(\omega t - /v_{G1} /)$ with \hat{v}_{G1} and $/v_{G1} /$ given. The principle consists, by considering the relations presented in II.2.2, in proceeding, after an initialization phase, with successive iterations. The latter will be distinguished by assigning the variables an upper index by brackets "j" which will take the values 0, 1, 2, ..., j_{max} . This value of j_{max}

will be defined by the user according to the desired accuracy on the response sought from the behavior of the MC. Let us introduce the set $S(j)$ consisting of the numerical values of $b^{(j)}$, $\mu_r^{(j)}$, $i_{\mu}^{(j)}$, $i_{ll}^{(j)}$, $i_{ll}^{(j)}$ and $u^{(j)}$. The calculation steps break down as follows:

Initialization phase (0). $e^{(0)} = v_{G1}$ is first imposed that leads to $S^{(0)}$.

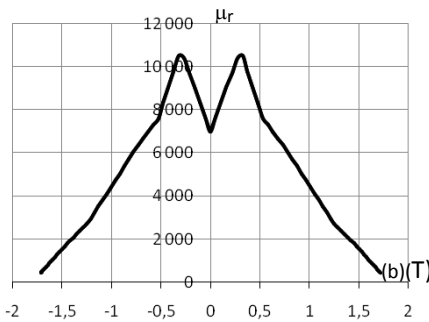


Fig. A1: $\mu_r(b)_{Th}$ Characteristic

Z↓	$\mu_r, Z-1$	μ_r, Z	$b_{Lim, Z-1}$	$b_{Lim, Z}$	α_z	β_z
1	7000	10800	0,00	0,30	7000	12666,7
2	10800	7600	0,30	0,53	14973,9	-13913,0
3	7600	6250	0,53	0,75	10852,3	-6136,4
4	6250	2700	0,75	1,25	11575,0	-7100,0
5	2700	1800	1,25	1,45	8325,0	-4500
6	1800	20	1,45	1,80	9174,3	-5085,7

TA1 : Characterization of $\mu_r(b)_{Th}$ segments

A2.2) Results. By fixing $V_{G1} \approx 19,03V$, \hat{b}_1 is of the order of 1,65T. By adopting a temporal reference such that at $t=0$, $v_{G1}/=0$, the numerical values obtained following the implementation of SAM, which is referenced SAM_{Th}, are grouped together in TA2. These use 3 decimals to characterize the peak values (noted γ_k^{\wedge} instead of $\hat{\gamma}_k$) and the powers and 2 decimals for the phase shifts expressed in "°".

As regards the structuring of TA2, the penultimate column shows either the rmss or mean values (denoted $\langle \rangle$) of the variables, either the sums over k (denoted Σk) of the powers. In the last column are grouped the THDs of the variables. On the other hand, TA2 is split into several parts:

- Line 1: numerical values relating to the various criteria concerning $v_G^{j_{max}}$.
- Part 1 (lines 4 to 20): FSs coefficients of $v_G^{j_{max}}$, v, i, e, b, u, i_{il} , i_{μ} and $/i_{\mu k}/e_k/$.
- Part 2 (lines 22 to 27) : FSs coefficients of i'_{μ} and i''_{μ} components of i_{μ} (see III.1).
- Part 3 (lines 29 à 38) : FSs coefficients of powers relative to the external and internal variables.
- Part 4 (lines 40 à 44) : FSs coefficients of powers conveyed by par i_{μ} (see III.1).
- Line 45 : numerical values of $Q''_{\mu 1(t)}$ and of the sum $Q'_{\mu 1} + Q''_{\mu 1(t)}$ (see III.3.2).
- Line 46 : numerical values of $X'_{\mu 1}$ and $X''_{\mu 1(t)}$ reactances (see III.3.2).
- Part 5 (lines 48 à 52) : FSs coefficients of μ_r and $10^4 \eta_r$ (see II.2.1)

Fig. A2 presents several plots: (a) to (d) temporal evolutions on T of different variables - (e) cycle b(i).

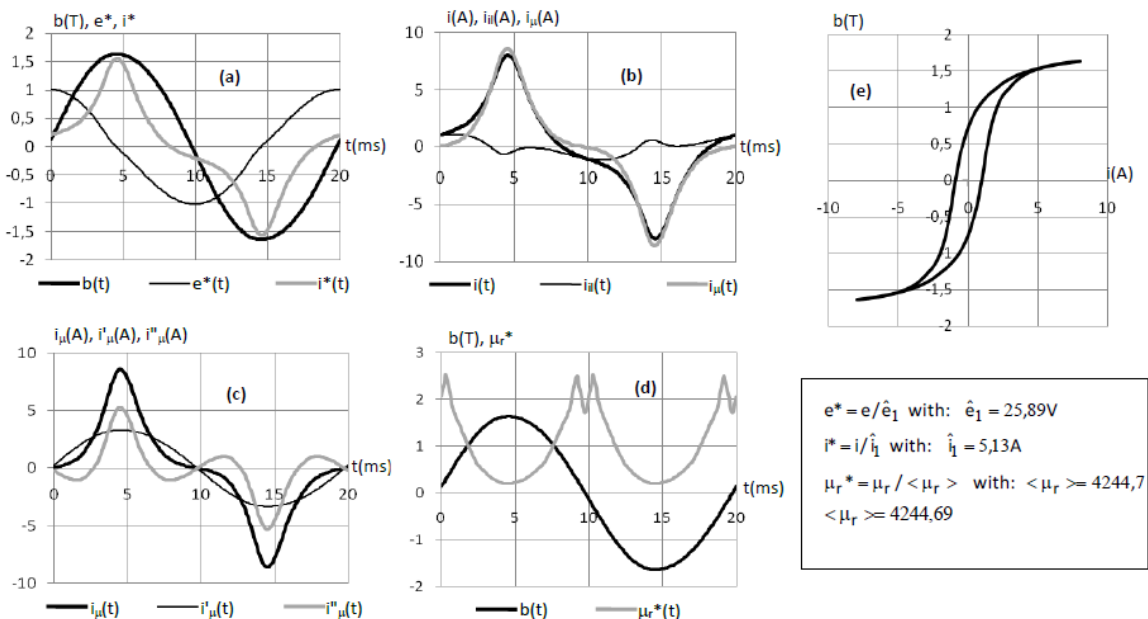


Fig. A2: SAM_{Th}: Theoretical case relating to $\hat{b}_1 = 1,65T$ - (a), (b), (c) and (d): Temporal evolutions of the main variables - (e): Cycle b(i)

Line 1 of TA2 shows that the value of $j_{max}=30$ adopted for this determination is more than sufficient insofar as the values which characterize the 3 constraints probably only correspond mainly to numerical errors.

TA2) SAM _{Th} - Data: $r=0,5\Omega$, $x=0,09\Omega$, $r_p=0,37\Omega$, $x_p=0,08\Omega$, $R_{ll}=31,8\Omega$, $R_{lk}=2,5\Omega \forall k>1$ - $V_{G1}=19,032V$, $b_1=1,65T$ - Ref : $V_{G1}/=0^\circ$																									
Tests on $v_G^{j_{max}}$: THD ($v_G^{j_{max}}$) = $1,28 \cdot 10^{-5}$ (%) - $\delta v_G^{j_{max}} = -6,32 \cdot 10^{-10}$ (V), $\delta / v_G^{j_{max}} = 1,99 \cdot 10^{-9}$ (°)																									
1	k												1	3	5	7	9	11	13	15	17	19	21		
2	Part 1 : External and internal variables												rms	THD(%)											
3	$\hat{v}_{Gk}^{j_{max}}$ (V)	26,915	0,000	0,000	0,000	0,000	0,000	0,000	0,000	0,000	0,000	0,000	0,000	0,000	0,000	0,000	19,032	0,00							
4	$/v_G^{j_{max}}$ (°)	0,00	96,05	148,65	260,89	24,11	154,24	-84,56	24,01	124,88	215,81	263,06													
5	v_k^{\wedge} (V)	26,695	0,254	0,090	0,037	0,017	0,006	0,003	0,002	0,001	0,001	0,000	18,877	1,02											
6	$/v_k^{\wedge}$ (°)	-1,35	60,42	214,57	7,98	164,85	-41,51	32,40	172,91	140,90	-78,03	135,06													
7	i_k^{\wedge} (A)	5,132	1,904	0,648	0,248	0,107	0,038	0,016	0,010	0,005	0,004	0,001	3,903	36,78											
8	$/i_k^{\wedge}$ (°)	74,52	253,40	55,53	216,09	19,19	178,16	256,61	40,94	12,17	156,09	10,97													
9	e_k^{\wedge} (V)	25,892	1,082	0,435	0,198	0,101	0,042	0,020	0,014	0,008	0,007	0,002	18,328	4,58											
10	$/e_k^{\wedge}$ (°)	-5,21	45,06	193,66	-15,25	141,22	-64,58	10,33	151,97	121,10	263,33	116,91													
11	b_k^{\wedge} (T)	1,650	0,023	0,006	0,002	0,001	0,000	0,000	0,000	0,000	0,000	0,000	1,167	1,44											
12	$/b_k^{\wedge}$ (°)	84,79	135,06	-76,34	74,75	231,22	25,42	100,33	241,97	211,10	-6,67	206,91													
13	u_k^{\wedge} (V)	2,607	1,082	0,435	0,198	0,101	0,042	0,020	0,014	0,008	0,007	0,002	2,026	41,47											
14	$/u_k^{\wedge}$ (°)	64,31	225,06	13,66	164,75	-38,78	115,42	190,33	-28,03	-58,90	83,34	-63,13													
15	i_{ik}^{\wedge} (A)	0,814	0,433	0,174	0,079	0,040	0,017	0,008	0,006	0,003	0,003	0,001	0,667	50,41											
16	$/i_{ik}^{\wedge}$ (°)	-5,21	45,06	193,66	-15,25	141,22	-64,58	10,33	151,97	121,10	263,33	116,91													
17	i_{jk}^{\wedge} (A)	5,051	2,295	0,786	0,304	0,133	0,048	0,021	0,014	0,007	0,005	0,002	3,969	43,62											
18	$/i_{jk}^{\wedge}$ (°)	83,64	248,26	47,03	204,32	4,27	160,23	235,84	17,50	-13,76	127,86	-19,33													
19	$/i_{jk}/e_k^{\wedge}$ (°)	88,85	203,20	-146,63	219,57	-136,95	224,82	225,51	-134,47	-134,85	-135,47	-136,24													
20	Part 2: i_{ij} components												rms	THD(%)											
21	i_{jk}^{\wedge} (A)	3,342	0,047	0,011	0,004	0,001	0,000	0,000	0,000	0,000	0,000	0,000	2,363	1,44											
22	$/i_{jk}^{\wedge}$ (°)	84,79	135,06	-76,34	74,75	231,22	25,42	100,33	241,97	211,10	-6,67	206,91													
23	$/i_{jk}/e_k^{\wedge}$ (°)	90,00	90,00	-270,00	90,00	90,00	90,00	90,00	90,00	90,00	-270,00	90,00													
24	i_{ij}^{\wedge} (A)	1,711	2,313	0,792	0,306	0,134	0,048	0,021	0,014	0,007	0,005	0,002	2,124	82,19											
25	$/i_{ij}^{\wedge}$ (°)	81,40	249,32	47,71	204,85	4,72	160,64	236,22	17,87	-13,40	128,20	-19,00													
26	$/i_{ij}/e_k^{\wedge}$ (°)	86,60	204,26	-145,95	220,10	-136,49	225,21	225,89	-134,10	-134,49	-135,06	-136,35													
27	Part 3: Powers												Σk												
28	P_{Gk} (W)	18,439	0,000	0,000	0,000	0,000	0,000	0,000	0,000	0,000	0,000	0,000	18,439												
29	Q_{Gk} (VAR)	66,563	0,000	0,000	0,000	0,000	0,000	0,000	0,000	0,000	0,000	0,000	66,563												
30	P_{extk} (W)	16,727	-0,236	-0,027	-0,004	-0,001	0,000	0,000	0,000	0,000	0,000	0,000	16,459												
31	Q_{extk} (VAR)	66,432	-0,054	-0,010	-0,002	-0,001	0,000	0,000	0,000	0,000	0,000	0,000	66,364												
32	p_k (W)	6,585	0,907	0,105	0,015	0,003	0,000	0,000	0,000	0,000	0,000	0,000	7,616												
33	q_k (VAR)	1,185	0,489	0,094	0,019	0,005	0,001	0,000	0,000	0,000	0,000	0,000	1,793												
34	P_{lk} (W)	10,541	0,234	0,038	0,008	0,002	0,000	0,000	0,000	0,000	0,000	0,000	10,823												
35	P_{mkk} (W)	11,853	-0,907	-0,105	-0,015	-0,003	0,000	0,000	0,000	0,000	0,000	0,000	10,823												
36	Q_{mkk} (VAR)	65,378	-0,489	-0,094	-0,019	-0,005	-0,001	0,000	0,000	0,000	0,000	0,000	64,770												
37	$P_{lk}+p_k$ (W)	17,126	1,141	0,143	0,023	0,005	0,001	0,000	0,000	0,000	0,000	0,000	18,439												
38	Part 4: Power components relating to i_{ij} - Particularity: $P_{jk}=P_{ij}^* \forall k$												Σk												
39	P_{jk} (W)	1,313	-1,141	-0,143	-0,023	-0,005	-0,001	0,000	0,000	0,000	0,000	0,000	0,000												
40	Q_{jk} (VAR)	65,378	-0,489	-0,094	-0,019	-0,005	-0,001	0,000	0,000	0,000	0,000	0,000	64,770												
41	Q_{jk}^* (VAR)	43,266	0,025	0,002	0,000	0,000	0,000	0,000	0,000	0,000	0,000	0,000	43,294												
42	Q_{ij}^* (VAR)	22,112	-0,514	-0,097	-0,020	-0,005	-0,001	0,000	0,000	0,000	0,000	0,000	21,476												
43	$q_k+Q_{jk}^*$ (VAR)	44,451	0,514	0,097	0,020	0,005	0,001	0,000	0,000	0,000	0,000	0,000	45,087												
44	$Q_{ij}^*+Q_{ij}^*=21,476$ (VAR)												$Q_{ij}^*+Q_{ij}^*=64,743$ VAR												
45	Magnetizing reactances: $X_{ij}^*=7,747\Omega$ - $X_{ij}^*+X_{ij}^*=15,608\Omega$																								
46	Part 5: Magnetic material characterisation																								
47	$2h$	2	4	6	8	10	12	14	16	18	20	22	<>	THD(%)											
48	μ_{r2h}^{\wedge} (°)	4176,68	960,88	91,57	165,64	222,25	284,56	355,26	345,77	289,09	232,91	164,93	4244,69	28,14											
49	$/\mu_{r2h}^{\wedge}$ (°)	-11,12	-16,04	-25,21	138,29	134,77	125,37	113,61	104,87	96,92	86,63	76,58													
50	$10^{4*} \eta_{r2h}^{\wedge}$ (°)	4,611	1,597	0,556	0,277	0,095	0,039	0,074	0,039	0,024	0,032	0,027	4,465	34,95											
51	$/\eta_{r2h}^{\wedge}$ (°)	166,70	-32,02	124,27	-71,39	73,91	262,96	-65,90	-75,75	-65,74	259,51	250,38													

TA2: Numerical data deduced from SAM_{Th} for theoretical case ($\hat{b}_1=1,65T$)

For convenience \hat{y}_k in TA2 is denoted y_k^{\wedge}

Références

- [1]. P. C. Sen, "Principles of electric machines and power electronics". John Wiley & Sons, TK2000.S44, 1989, 621.3, 88-5725, ISBN 0-471-85084-5.
- [2]. D. K. Rao, V. Kuptsov, "Effective Use of Magnetization Data in the Design of Electric Machines With Overfluxed Regions", IEEE Trans. on Magnetics, Vol. 51, N° 7, July 2015, DOI: 10.1109/TMAG.2015.2397398.
- [3]. L. Wang, F. Ding, D. Yang, K. Wang, B. Jiao, Q. Chen, "A fitting-extrapolation method of B-H curve for magnetic saturation applications", COMPEL, Vol. 42, N° 2, pp.

- 494-505, <https://doi.org/10.1108/COMPEL-01-2022-0021>.
- [4]. A. E. Umenei, Y. Melikhov, D. C. Jiles, "Models for extrapolation of magnetization data on magnetic cores to high fields", *IEEE Trans. on Magnetics*, Vol. 47, N° 12, pp. 4707-4711, Dec. 2011, DOI: 10.1109/TMAG.2011.2159616.
- [5]. L. Janicke, A. Kost, R. Merte, T. Nakata, N. Takahashi, K. Fujiwara, K. Muramatsu, "Numerical modeling for anisotropic magnetic media including saturation effects", *IEEE Trans. on Magnetics*, Vol. 33, N° 2, pp. 1788-1791, 1997, DOI: 10.1109/20.582622.
- [6]. F. de Leon, A. Farazmand, P. Joseph, "Comparing the T and π Equivalent Circuits for the Calculation of Transformer Inrush Currents", *IEEE Trans. on Power Delivery*, Vol. 27, N° 4, pp. 2390-2397, 2012, DOI: 10.1109/TPWRD.2012.2208229.
- [7]. K. W. Chen, S. T. Glad, "Estimation of the primary current in a saturated transformer", *Proceedings of the 30th IEEE Conference on Decision and Control*, Vol. 3, Dec. 1991, pp. 2363-2365, DOI: 10.1109/CDC.1991.261872.
- [8]. T. D. Kefalas, A. G. Kladas, "Analysis of transformers working under heavily saturated conditions in grid-connected renewable-energy systems", *IEEE Trans. on Industrial Electronics*, Vol. 59, N° 5, pp. 2342-2350, May 2012, DOI: 10.1109/TIE.2011.2161068.
- [9]. Q. C. Qu, "Precise magnetic property measurement on electrical sheet steels under deep saturation", *IEEE Trans. on Magnetics*, Vol. 20, N° 5, Sept 1984, pp. 1717-1719, DOI: 10.1109/TMAG.1984.1063407.
- [10]. D. Miyagi, T. Yamazaki, D. Otome, M. Nakano, N. Takahashi, "Development of Measurement System of Magnetic Properties at High Flux Density Using Novel Single-sheet Tester", *IEEE Trans. on Magnetics*, Vol. 45, N° 10, pp. 3889-3892, Oct. 2009, DOI: 10.1109/TMAG.2009.2022332.
- [11]. Q. Tang, P. Anderson, Z. D. Wang, A. Moses, P. Jarman, "Measurement of magnetic properties of electrical steels at high flux densities using an improved single sheet tester", *International Symposium on High Voltage Engineering*, Jan. 2013, DOI:10.13140/2.1.5025.5046.
- [12]. Y. Wang, X. Zhong, X. Chen, "Influence of saturation levels on transformer equivalent circuit model", *Journal of Electrical Engineering*, Dec. 2021, Vol. 72, N° 6, pp. 381-387, DOI: <https://doi.org/10.2478/jee-2021-0054>.
- [13]. J. F. Brudny, "Saturated single phase magnetic circuit under sinusoidal voltage: Iron losses - definition of a new physical concept - equivalent schemes", *Elsevier, Int. Journal of Electrical Power & Energy Systems (IJEPES)*, Vol. 125, feb. 2021. <https://doi.org/10.1016/j.ijepes.2020.106381>.
- [14]. Ph. Guinic, J. F. Brudny, V. Costan, M. Dessoude, "Series voltage regulator with electronics protected against short-circuits by magnetic circuit-based decoupling using holes and windows", *Patent*, 2012, WO 012/126884.
- [15]. J. F. Brudny, Ph. Guinic, V. Costan, "Series current limiter using a magnetic circuit comprising holes and windows", *Patent*, W0/2012/126886, 27.09.2012, International Application No PCT/EP2012/054812.
- [16]. Dale S. L. Dolan; P. W. Lehn, "Analysis of a Virtual Air Gap Variable Reactor", 2007 *IEEE Power Electronics Specialists Conference*, DOI: 10.1109/PESC.2007.4342160.
- [17]. S. Magdaleno, C. P. Rojas, "Control of the magnetizing characteristics of a toroidal core using virtual gap", *Electronics, Robotics and Automotive Mechanics Conference (CERMA)*, Sept. 2010, pp. 540-545, DOI: 10.1109/CERMA.2010.121.
- [18]. J. F. Brudny, G. Parent, I. Naceur, "Characterization and Modeling of a Virtual Air Gap by Means of a Reluctance Network", *IEEE Trans. on Magnetics*, Vol. 53, N° 7, July 2017, DOI: 10.1109/TMAG.2017.2680402.
- [19]. J. Sievert, "The measurement of magnetic properties of electrical sheet steel - survey on methods and situation of standards", *Elsevier, Journal of Magnetism and Magnetic Material*, Vols 215-216, June 2000, pp. 647-651, [https://doi.org/10.1016/S0304-8853\(00\)00251-1](https://doi.org/10.1016/S0304-8853(00)00251-1).
- [20]. Ph. Marketos, S. Zurek, A. J. Moses, "A Méthod for Defining the Mean Path Length of the Epstein Frame", *IEEE Trans. on Magnetics*, Vol. 43, N° 6, June 2007, pp. 2755-2757, DOI : 10.1109/RMAG.2007.894124.
- [21]. H. Pfützner, G. Shilyashki, "Concept for industrially relevant magnetic power loss measurements by Single Sheet Tester and Epstein Frame Testers", *CIGRE Sci. & Eng.* 9, pp. 95-109, 2017.

- [22]. G. Shilyashki, H. Pfützner, "Consistent Measurements of Magnetic Energy Losses by a Low-Mass, High-Frequency Single Sheet Tester", *Academia Letters*, 2022, ISSN: 2771-9359, <https://doi.org/10.20935/AL5263>.
- [23]. S. E. Zirka, Y. I. Moroz, C. M. Artury, "Once again about the Steinmetz transformer model and the ongoing subdivision of its leakage inductance", *COMPEL*, October 11 01 22, ISSN: 0332-1649.
- [24]. X. Chen, "Negative Inductance and Numerical Instability of the Saturable Transformer Component in EMTP", *IEEE Trans. on Power Delivery*, Vol. 15, N° 4, pp. 1199- 1204, Oct. 2000, DOI: 10.1109/61.891503.
- [25]. P. S. S. Holenarsipur, N. Mohan, V. D. Albertson, J. Cristofersen, "Avoiding the use of negative inductances and resistances in modeling three-winding transformers for computer simulations", *IEEE Power Engineering Society, 1999 Winter Meeting (Cat. No.99CH36233)*, ISBN:0-7803-4893-1, DOI: 10.1109/PESW.1999.747338.
- [26]. M. Couvreur, E. De Jaeger, A. Robert, "Voltage Fluctuations and the Concept of Short-Circuit Power", *CIGRE 2000*, report 13/14/36-08.
- [27]. G. Bertotti, "General properties of power losses in soft ferromagnetic materials", *IEEE Trans. on Magnetics*, Vol. 24, N° 1, Jan. 1998, pp. 621-630, DOI: 10.1109/20.43994.
- [28]. G. Bertotti, M. Pasquale, "Physical interpretation of induction and frequency dependence of power losses in soft magnetic materials", *IEEE Trans. on Magnetics*, Vol. 28, N° 5, Sept. 1992, pp. 2787-2789, DOI: 10.1109/20.179627.
- [29]. M. Amar, R. Kaczmarek, "A general formula for prediction of iron losses under non sinusoidal voltage waveform", *IEEE Trans. on Magnetics*, Vol. 31, N° 5, Sept. 1995, pp. 2504-2509, DOI: 10.1109/20.406552.
- [30]. S. Steentjes, G. von Pfingsten, M. Hombitzer, K. Hameyer, "Iron-Loss Model With Consideration of Minor Loops Applied to FE-Simulations of Electrical Machines", *IEEE Trans. on Magnetics*, Vol. 49, N° 7, Jul. 2013, DOI: 10.1109/TMAG.2013.2244072.
- [31]. P. Brissoneau, "Magnétisme et matériaux magnétiques pour l'électrotechnique", Hermès, Paris 1997, ISBN 2-86601-579-7.
- [32]. IEC: 1996+A1:2008 - 60404-2, "Part 2: Methods of measurement of the magnetic properties of electrical steel strip and sheet by means of an Epstein tester".
- [33]. M. Cossale, G. Bramerdorfer, G. Goldbeck, M. Kitzberger, D. Andessner, W. Amrhein, "Modeling the Degradation of Relative Permeability in Soft Magnetic Materials", *IEEE Transportation Electrification Conference and Expo (ITEC)*, 2018, DOI: 10.1109/ITEC.2018.8450202.
- [34]. ArcelorMittal M400-50A data sheet.
- [35]. J. F. Brudny, B. Cassoret, R. Lemaître, J. N. Vincent, "Magnetic core and use of magnetic core for electrical machines", *WO Patent Application WO2009/030779*, July 2009.
- [36]. S. Lopez, B. Cassoret, J. F. Brudny, L. Lefebvre, J. N. Vincent, "Grain oriented Steel Assembly Characterization for the Development of High Efficiency AC Rotating Electrical Machines", *IEEE Trans. on Magnetics*, Vol. 45, N° 10, Oct. 2009, pp. 4161- 4164, DOI: 10.1109/TMAG.2009.2023243.
- [37]. S. Zurek, F. Al-Naemi, F. Marketos, A. J. Moses, "Anomalous B-H behaviour of electrical steels at very low flux density", *Journal of Magnetism and Magnetic Materials*, 320(20), October 2008, DOI:10.1016/j.jmmm.2008.04.041.